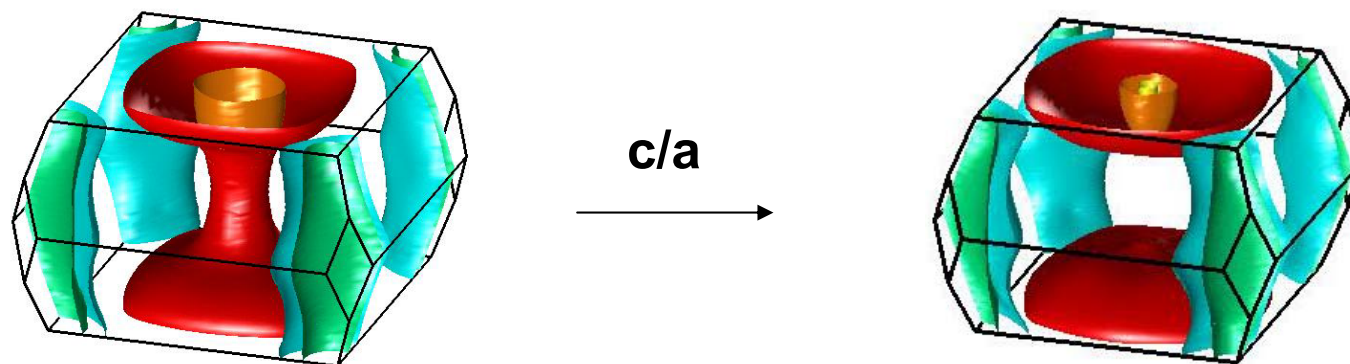


Topological changes of the Fermi surface and the effect of electronic correlations in iron pnictides



Amalia Coldea
Oxford University



Collaborators



Antony Carrington, Caroline Andrew, Jon Fletcher, A. Bangura
H. H. Wills Physics Laboratory, University of Bristol, UK



Ian Fisher, James Analytis, Jiun-Haw Chu, Hsueh-Hui Kuo
Geballe Laboratory for Advanced Materials, Stanford University, USA



S. Kasahara, H. Shishido, K. Hashimoto, T. Shibauchi, Y. Matsuda
Department of Physics, Kyoto University, Japan



Ross McDonald
National High Magnetic Field Laboratory,
Los Alamos National Laboratory, USA



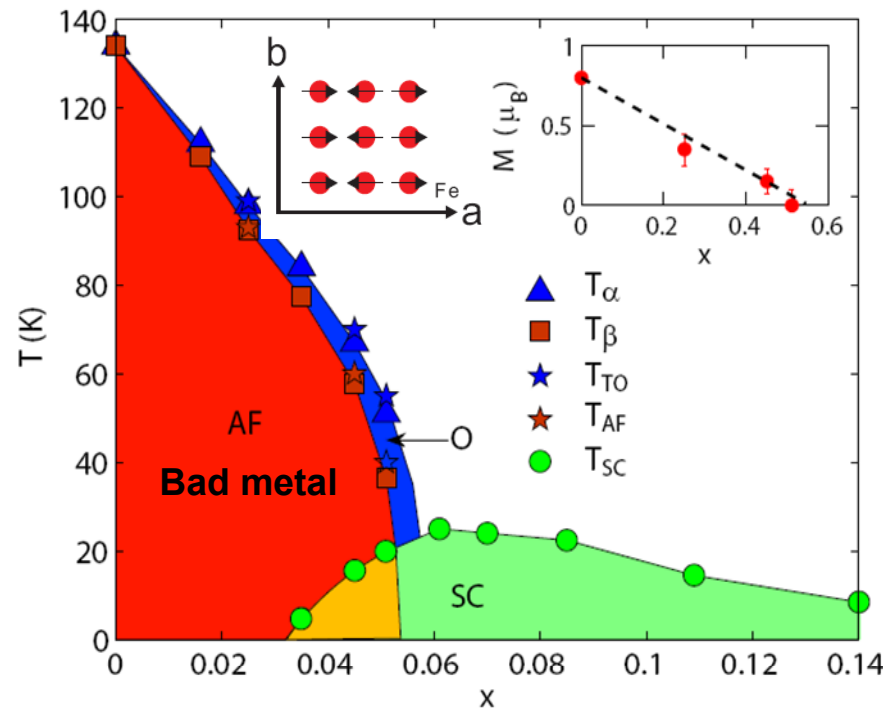
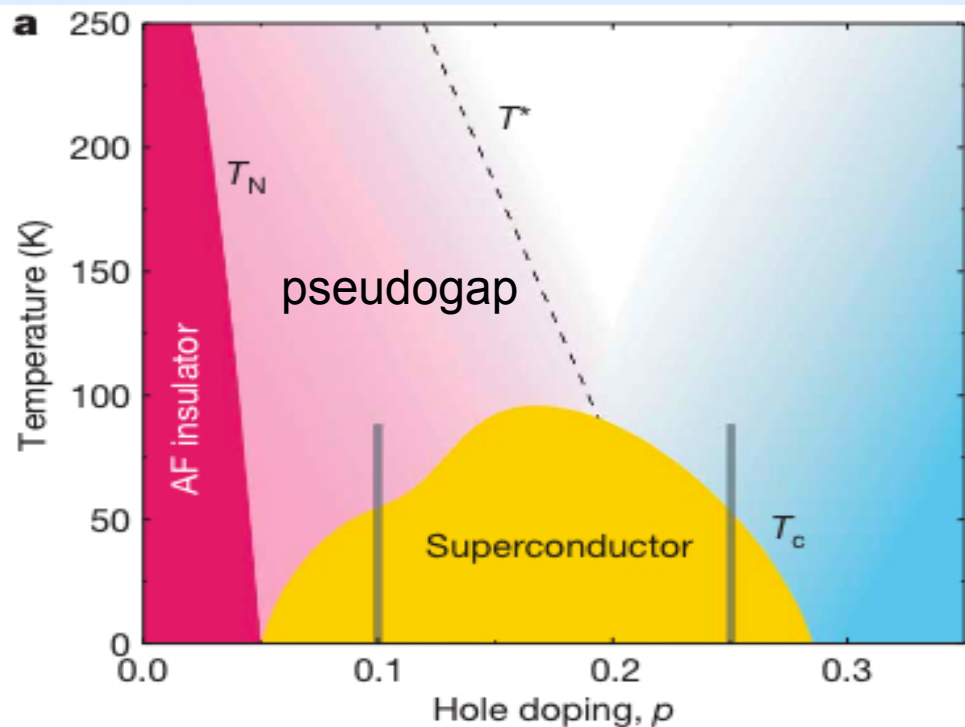
Alix McCollam
High Magnetic Field Laboratory,
Nijmegen, The Netherlands



D. Vignolles, C. Proust, B. Vignolle
Laboratoire National des Champs Magnétiques Intenses, Toulouse,
France



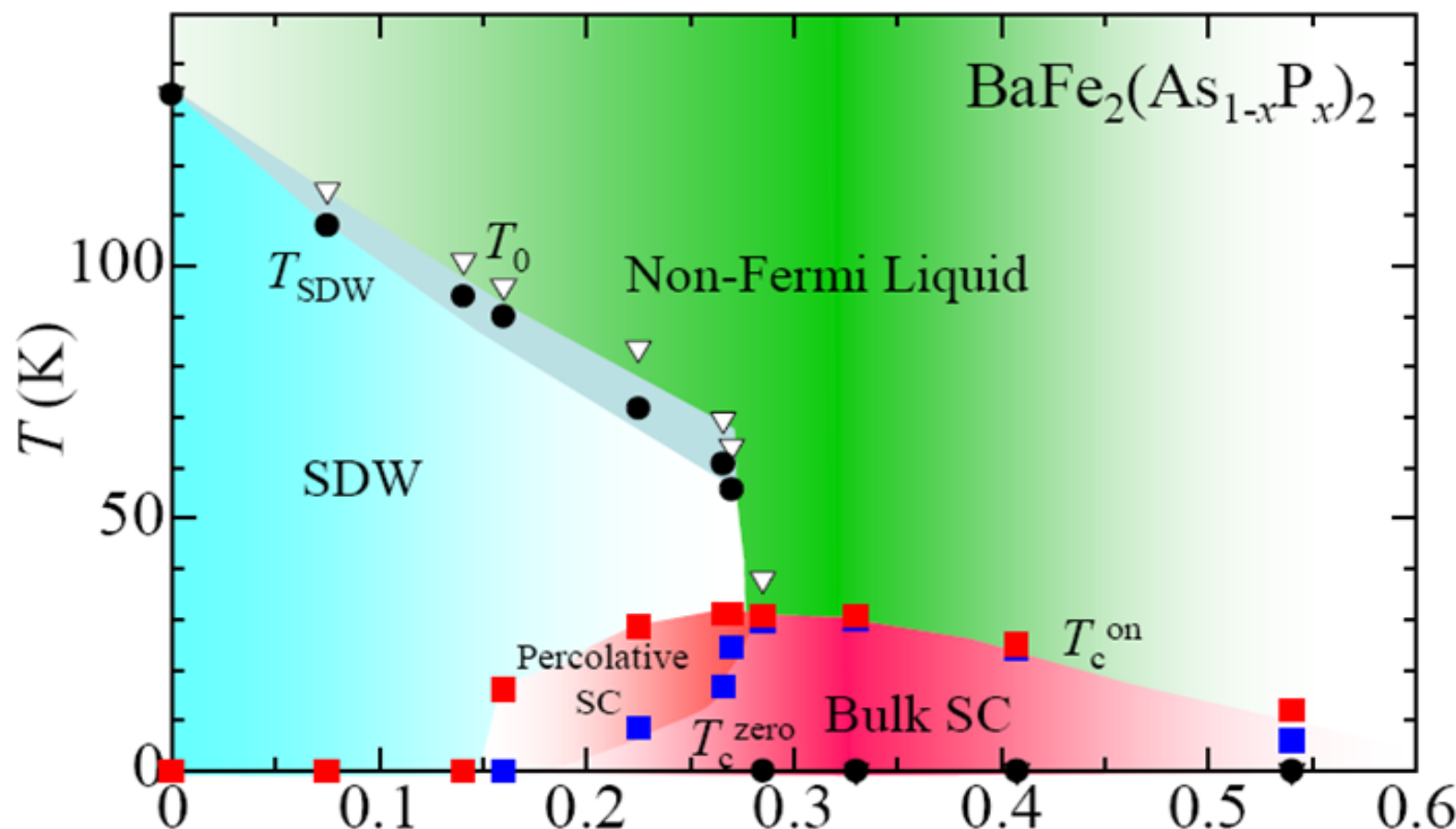
Phase diagrams: cuprates vs pnictides



- AFM ordering - Mott-insulator;
- Strong electronic correlations;
- pseudogap;
- $\text{Cu}^{2+} - \text{O}_{2p}$ $3d_{x^2-y^2}$ single band;

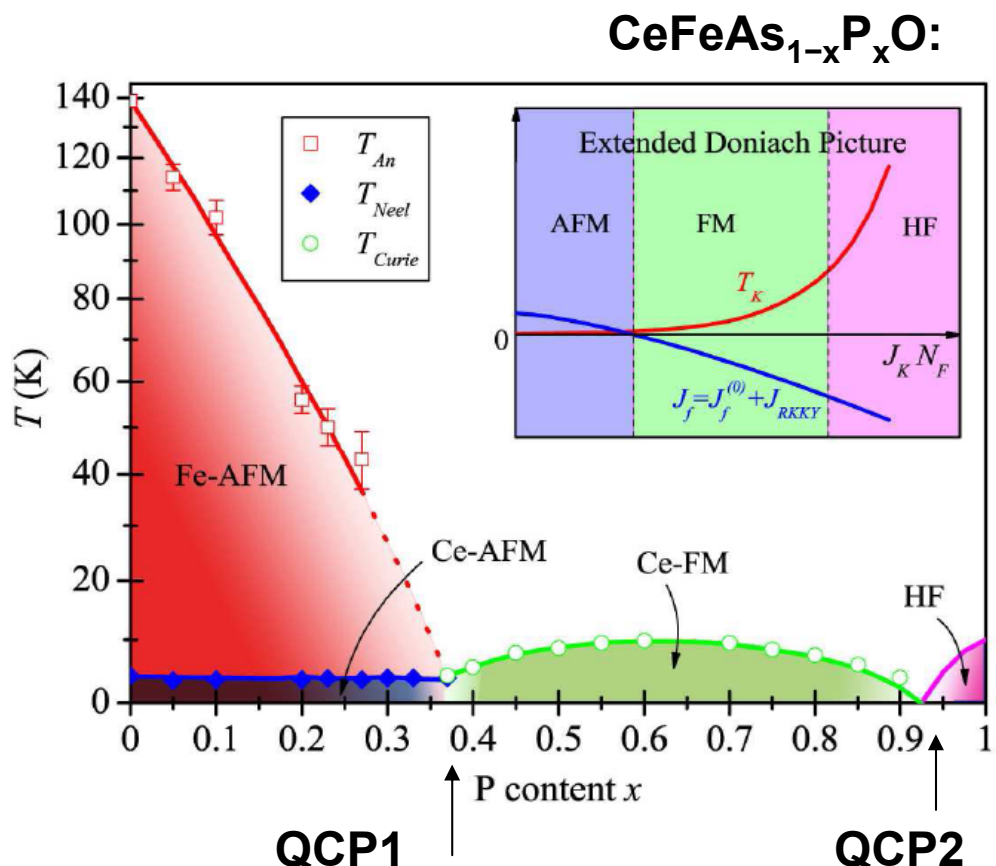
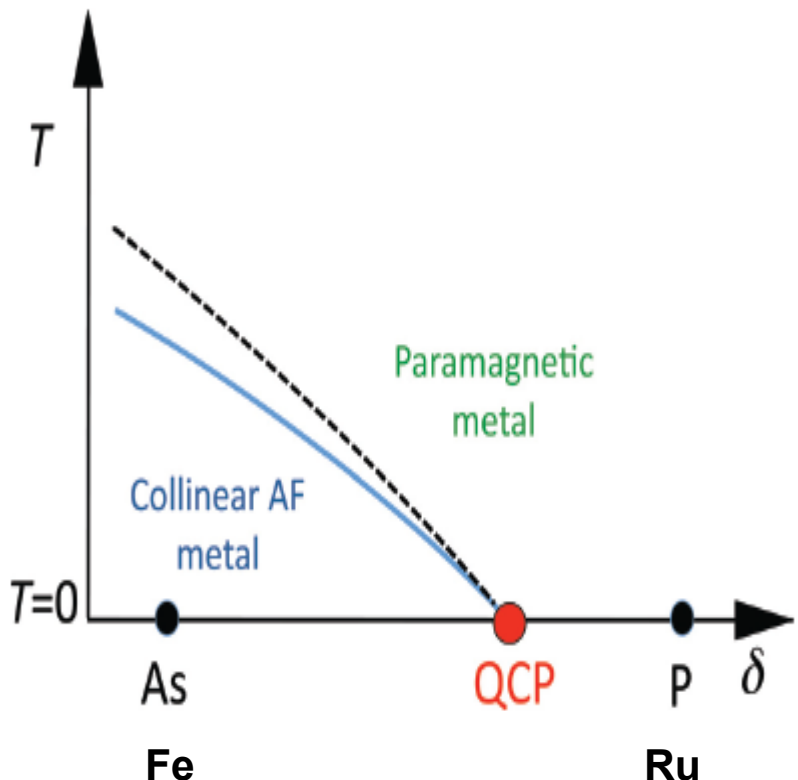
- AFM ordering – Bad metals;
- small carrier density ;
- Fe^{2+} - As^{3-} (d^6); all five d orbitals important;
- high density of states $N(\text{EF})$, prone to magnetic instabilities;

Effect of chemical pressure: P substitution



- suppression of magnetism and the presence of superconductivity through chemical substitutions: As replaced by P, or Fe replaced by 4d and 5d elements: Rh, Ir and Pd; other examples $\text{SrFe}_{1-x}\text{Ru}_x\text{As}_2$, $\text{LaFeAs}_{1-x}\text{P}_x\text{O}$ and $\text{EuFe}_2\text{As}_{2-x}\text{P}_x$.

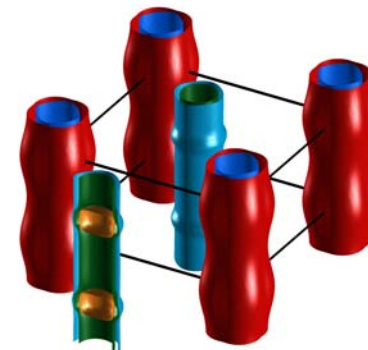
Criticality determined by As/P substitution



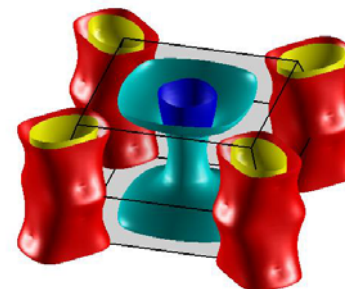
- suppression of magnetism by chemical substitution As/P, unique role of P-doping in suppressing the d -electron correlations.

Plan of my talk

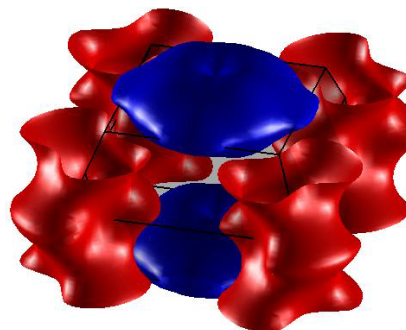
- Quantum oscillations to determine the Fermi surface and comparison with band structure calculations.
- the superconducting **LaFePO**; role of nesting ;
- Role of dimensionality on the Fermi surface: the case of **SrFe₂P₂**;
- Fermi surface shrinking and enhanced correlations in **BaFe₂(As_{1-x}P_x)₂**
- Topological change of the Fermi surface with c/a ratio: the case of **CaFe₂P₂**.
- Conclusions



111
LaFePO
 $T_c \sim 6\text{K}$



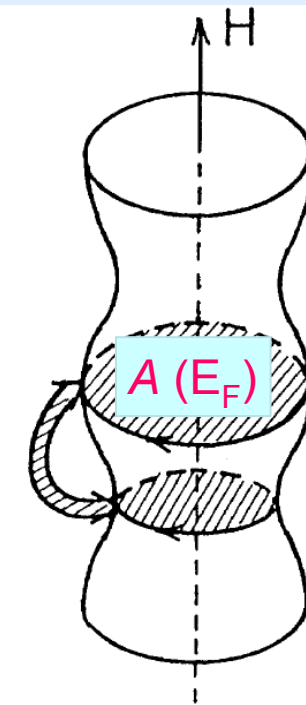
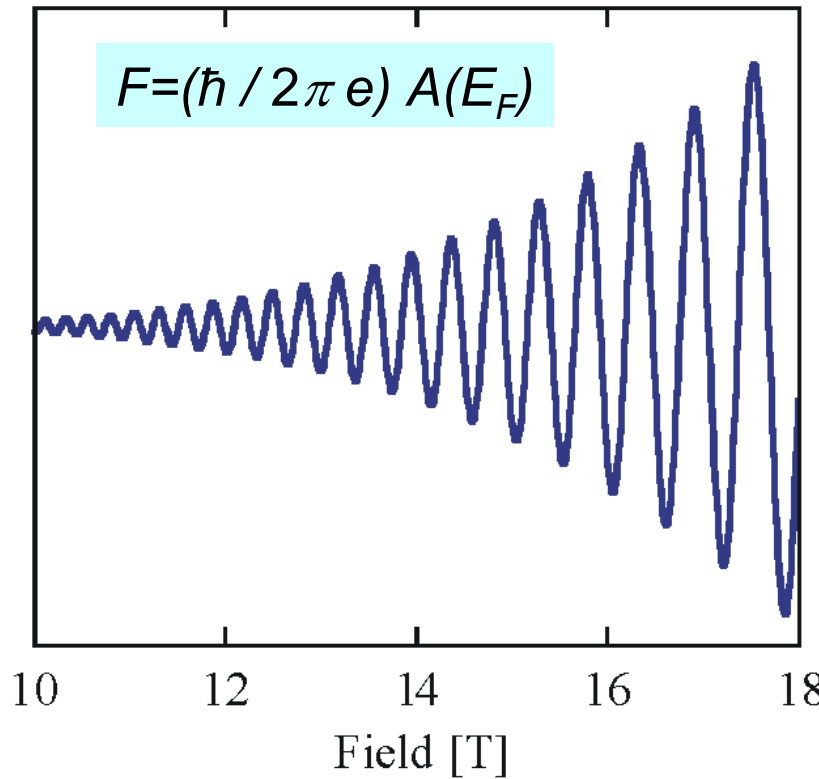
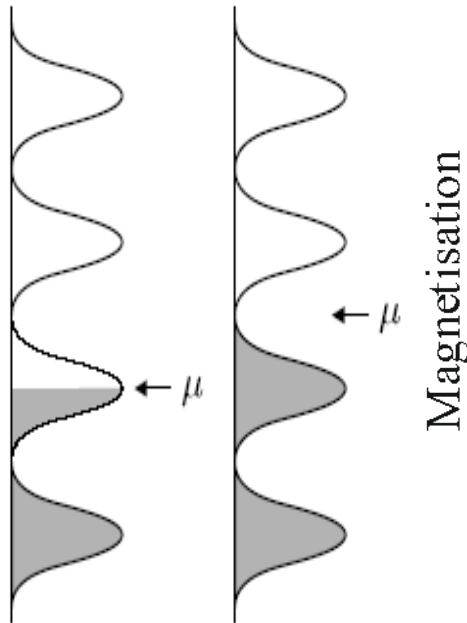
122
SrFe₂P₂
 $c/a=3.04$



122
CaFe₂P₂
 $c/a=2.65$

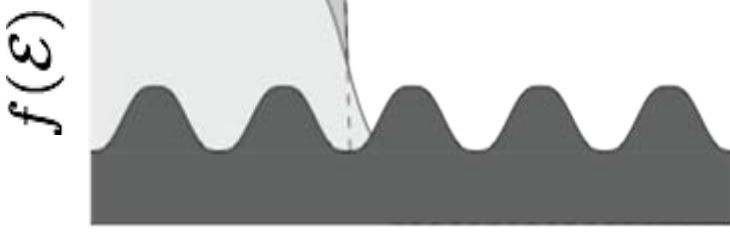
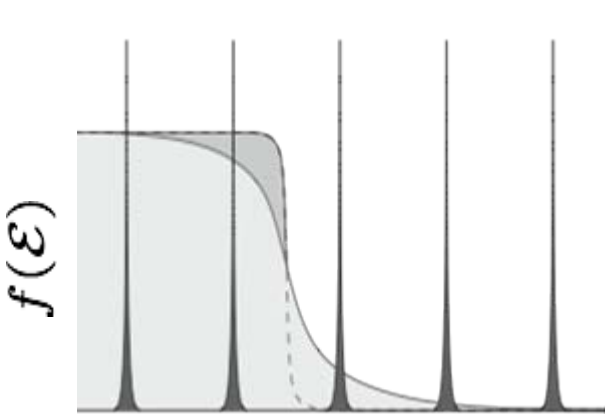
Quantum oscillations map out the Fermi surface

- oscillations of the density of states in magnetic field;



- ‘k-space microscopy’: 0.1% IBZ; 3D map of the Fermi surface;
- bulk probe; no sensitive to surface effects like ARPES;

Lifshitz-Kosevich formalism



$$M_{\text{osc}} \propto R_T R_D R_s R_{sc} \sin \left(\frac{2\pi F}{B} + \gamma \right)$$

Temperature - low temperatures

$$R_T = \frac{2\pi^2 p k_B T m^* / e \hbar B}{\sinh (2\pi^2 p k_B T m^* / e \hbar B)}$$

Finite scattering time – clean samples

$$R_D = e^{-2\pi^2 p k_B T_D m^* / e \hbar B}$$

Superconducting state –random vortex lattice

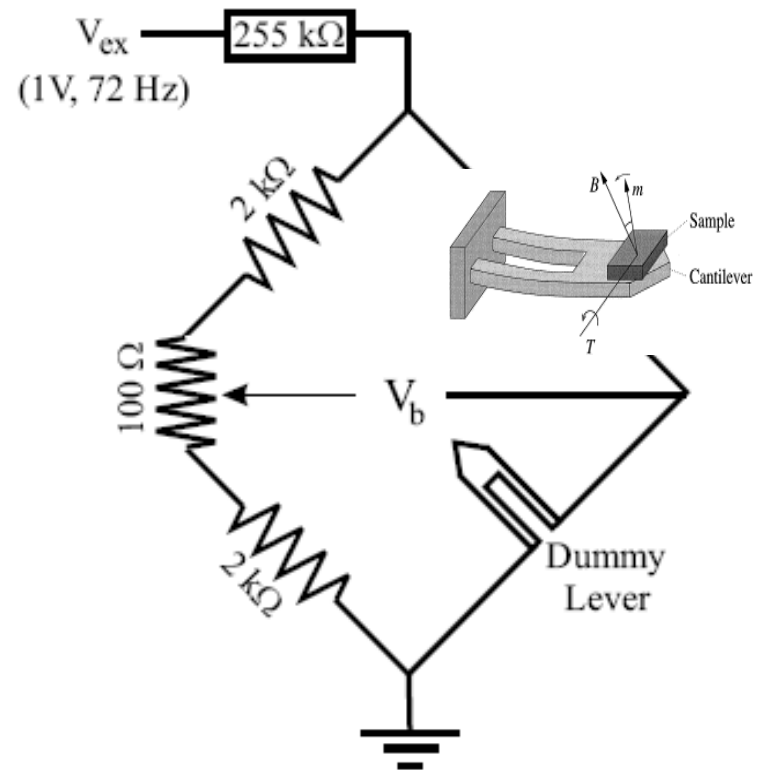
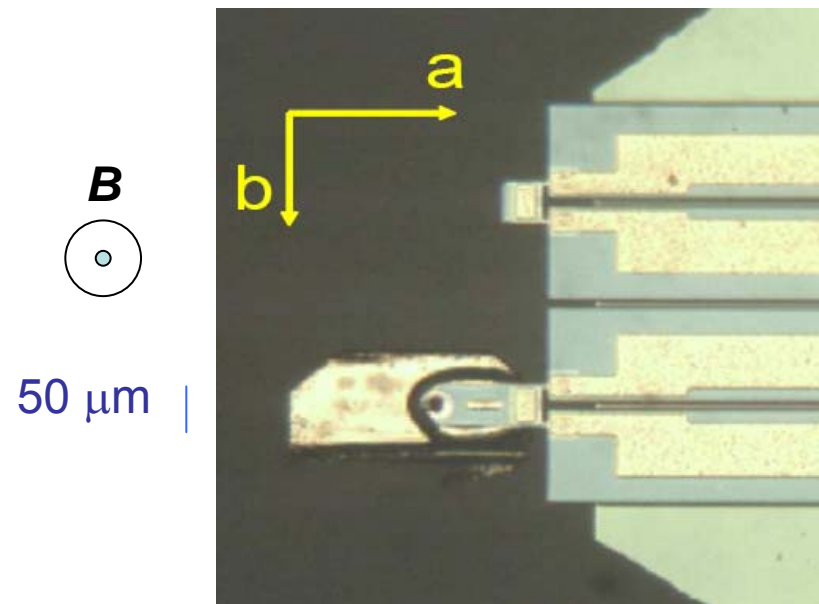
$$R_{SC} = \exp \left[-\pi^{\frac{3}{2}} \left(\frac{\Delta_E(B)}{\hbar \omega_c} \right)^2 \left(\frac{B}{F} \right)^{\frac{1}{2}} \right]$$

- extracted parameters: quasiparticle effective mass **m^* (band renormalization near the Fermi energy)**, scattering rates $\sim T_D = \hbar / (2p k_B t)$, spin-splitting factor **g^***

$$m^*/m_b = (1 + \lambda_{\text{el-ph}})(1 + \lambda_{\text{el-el}}) \sim 1 + \lambda_{\text{el-ph}} + \lambda_{\text{el-el}}$$

$$\frac{\Gamma m_b}{m_b} = \frac{1 + F_1^s / 3}{1 + F_0^a}$$

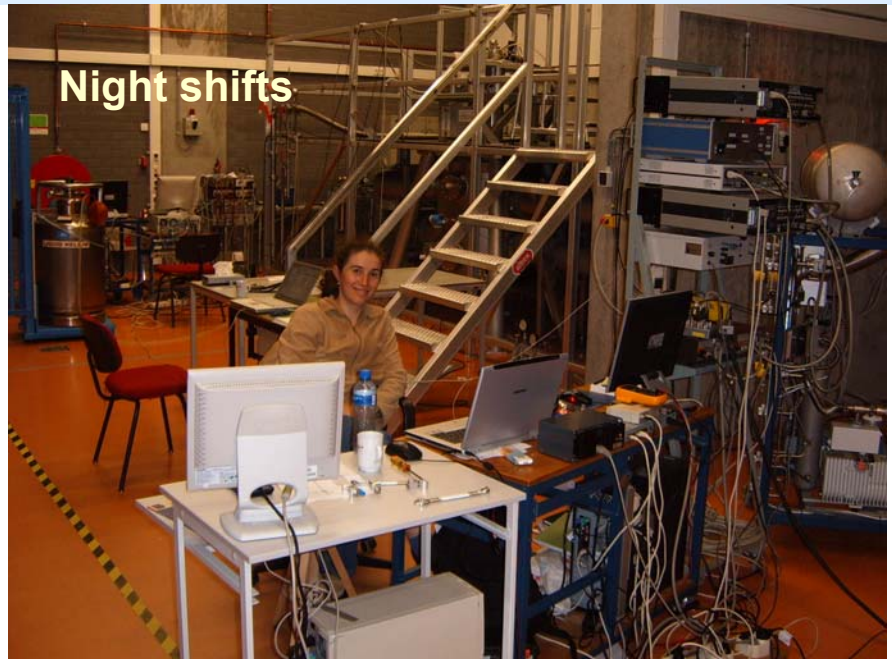
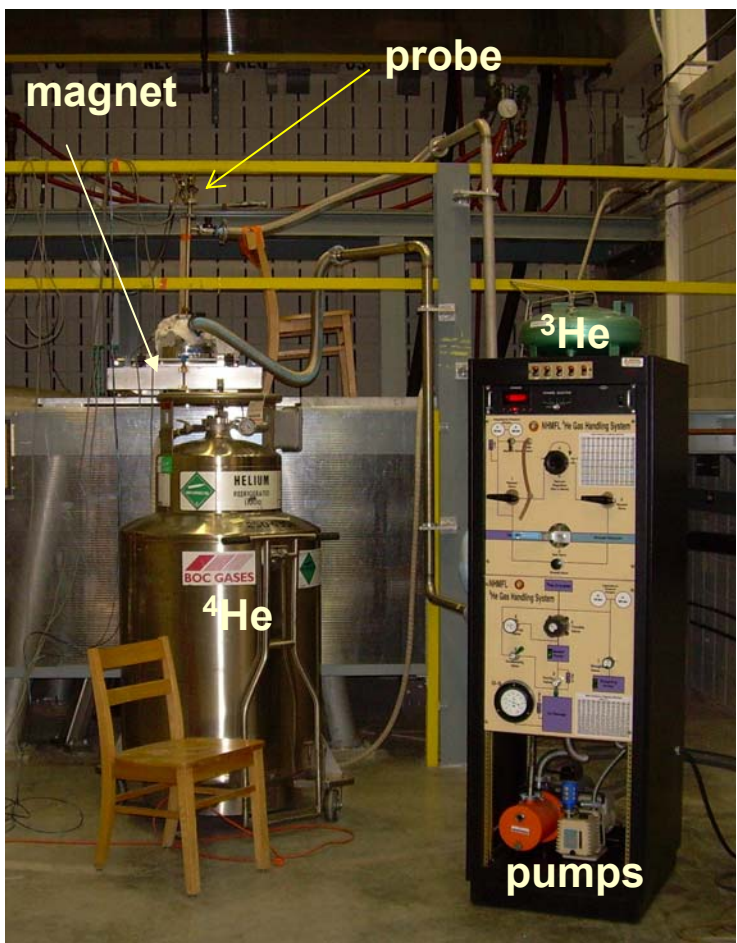
Torque measurements with AFM cantilevers



$$\tau = \mathbf{m} \times \mathbf{B}, \quad \tau = mB \sin(\theta)$$

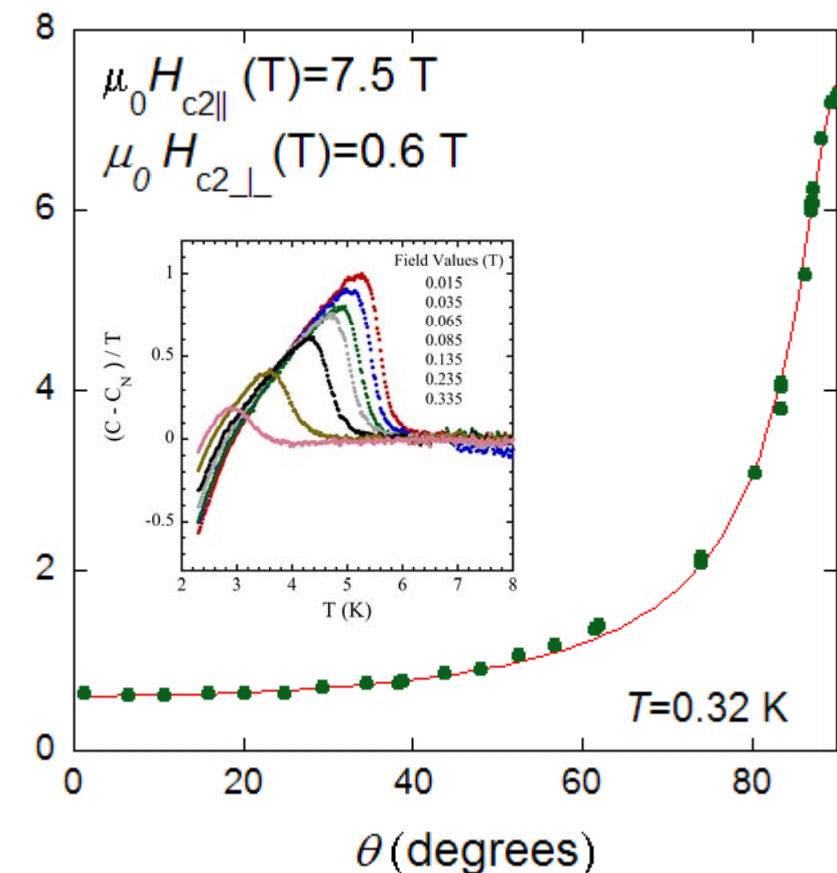
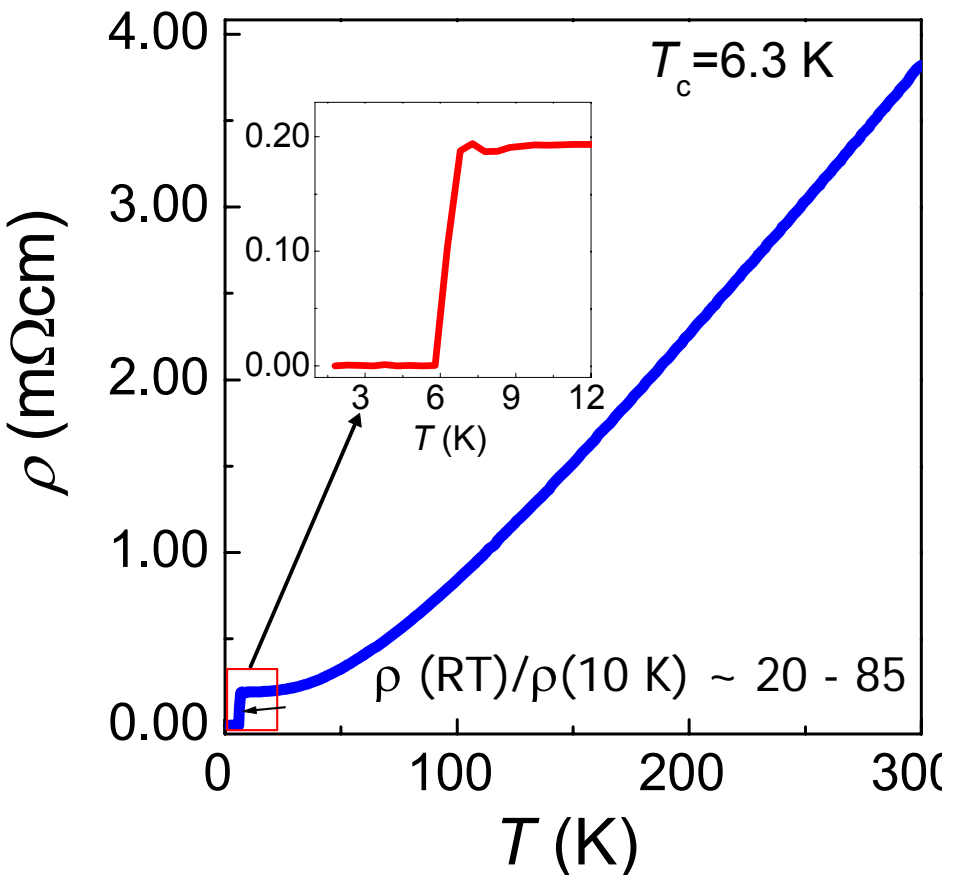
The resistance of the active piezocantilevers (SEIKO) is measured with respect to that of the dummy using a conventional ac Wheatstone bridge circuit.

High magnetic field and low temperatures



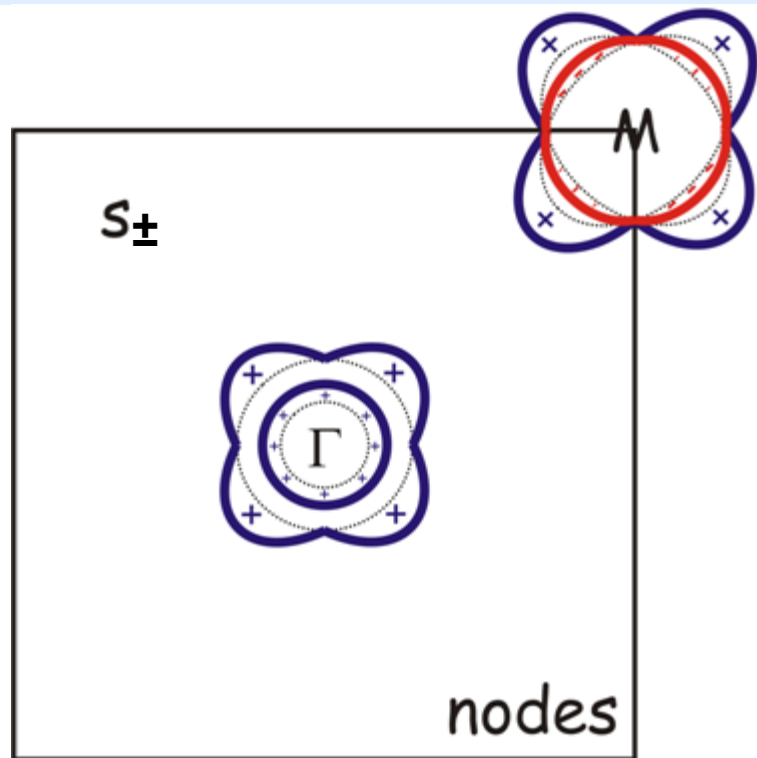
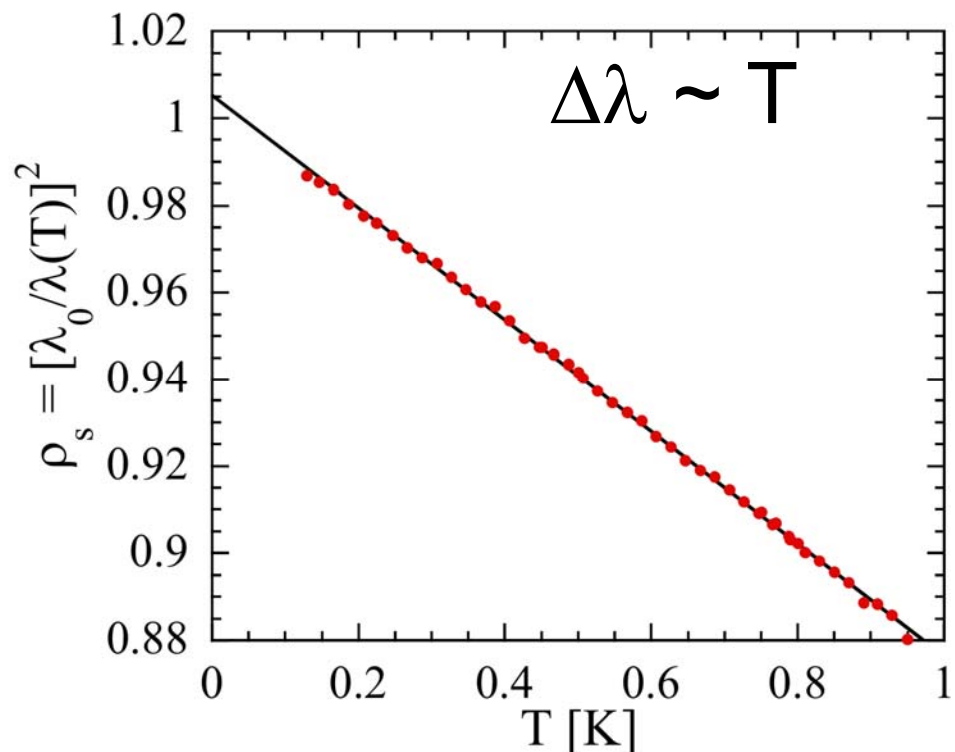
Low temperatures ($0.3 \text{ K} < T < 4 \text{ K}$), high magnetic fields ($0 < B < 55 \text{ T}$) at NHMFL, Tallahassee, USA, Nijmegen, The Netherlands and Toulouse, France; rotation in field ($-90^\circ < \theta < 90^\circ$);

Bulk superconductivity in LaFePO



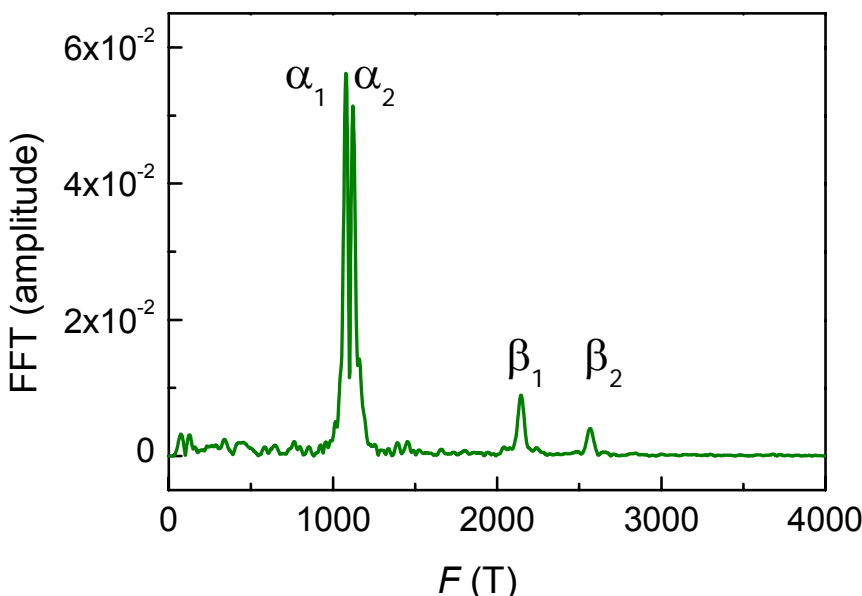
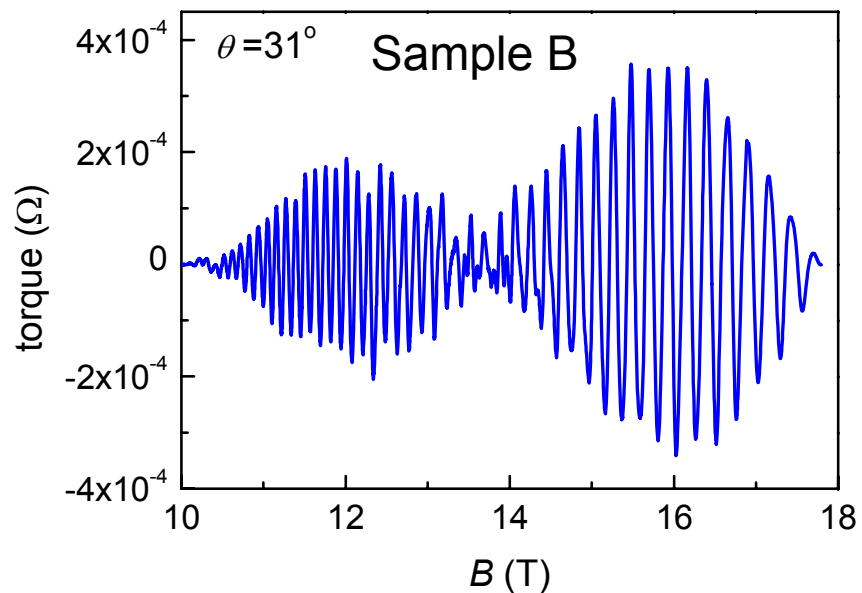
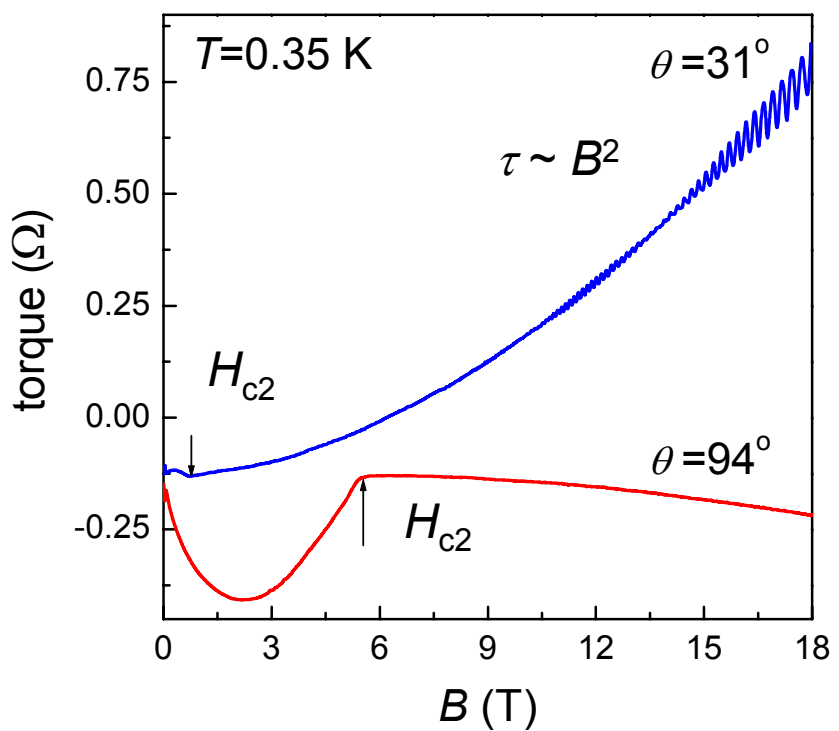
- High residual resistivity ratio: ~ 85 ; low H_{c2} ;
- Anomaly in specific heat: bulk superconductor; non-magnetic; $0.07 \mu_B/\text{Fe}$;
- reversible signal - weak pinning; **anisotropy ~ 10** ;

Superconducting order parameter with line nodes in LaFePO



- Clean superconductor: Superfluid density show linear dependence down to 100 mK suggesting the presence of **nodes** in the symmetry of the superconducting gap;

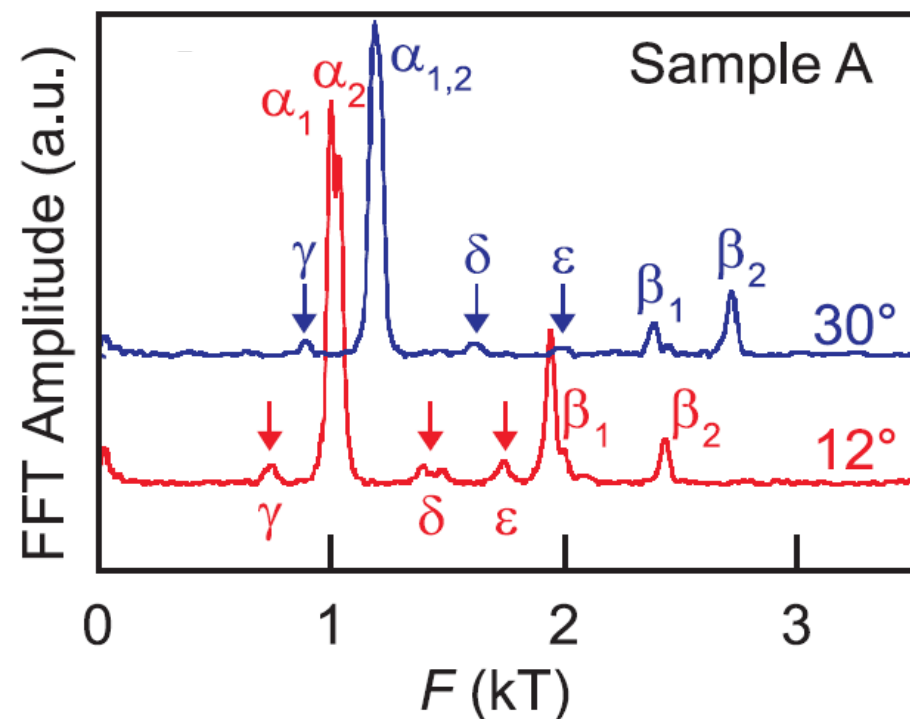
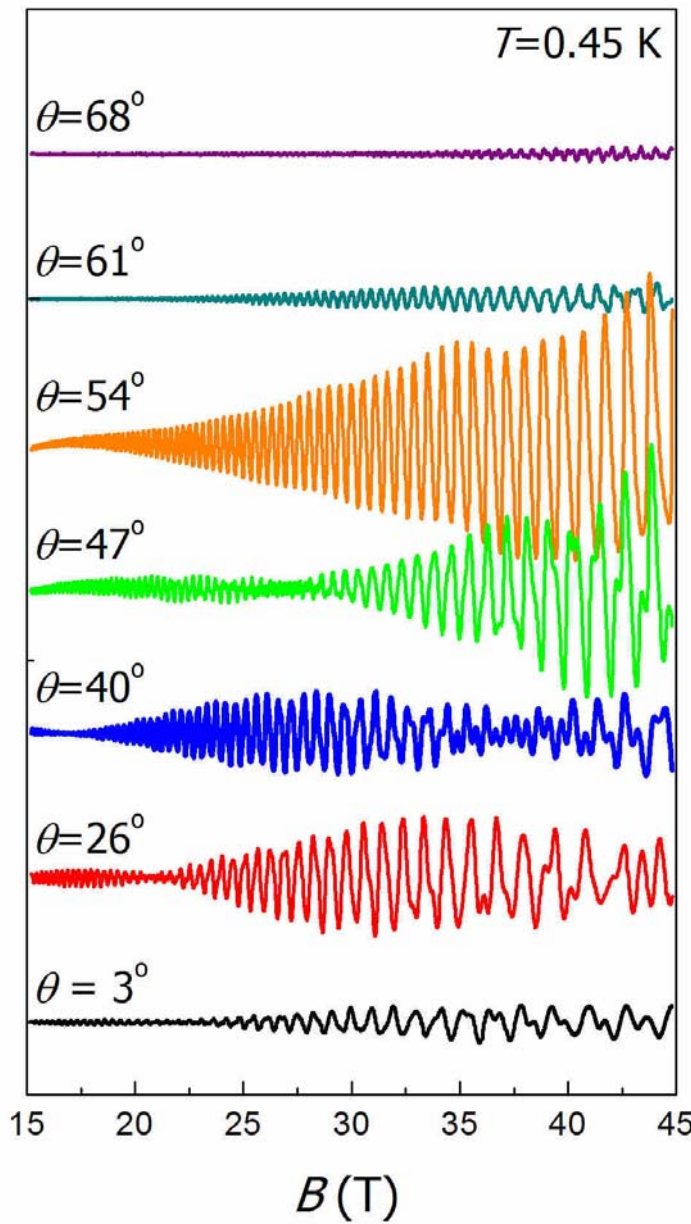
de Haas-van Alphen effect in LaFePO



- **high B :** normal state; oscillations periodic in inverse field, de Haas-van Alphen effect.
- $\tau \sim B^2$ –characteristic to a paramagnet;
- a simple corrugation of the Fermi cylinder leads to a **beat pattern** in the magnetization.

de Haas-van Alphen effect in LaFePO

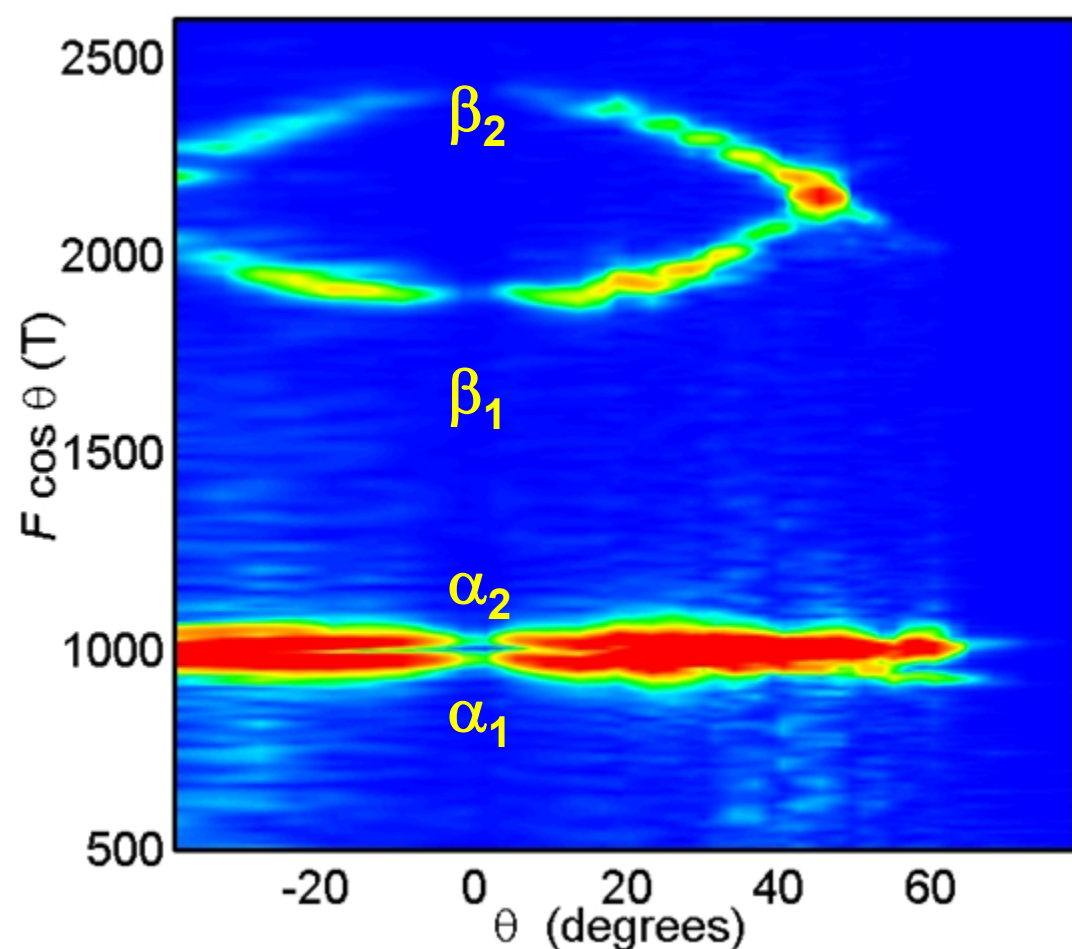
Torque (a.u.)



$$F = (\hbar / 2\pi e) A(E_F)$$

Different frequencies correspond to extremal areas of the Fermi surface perpendicular to the applied magnetic field for a particular orientation;

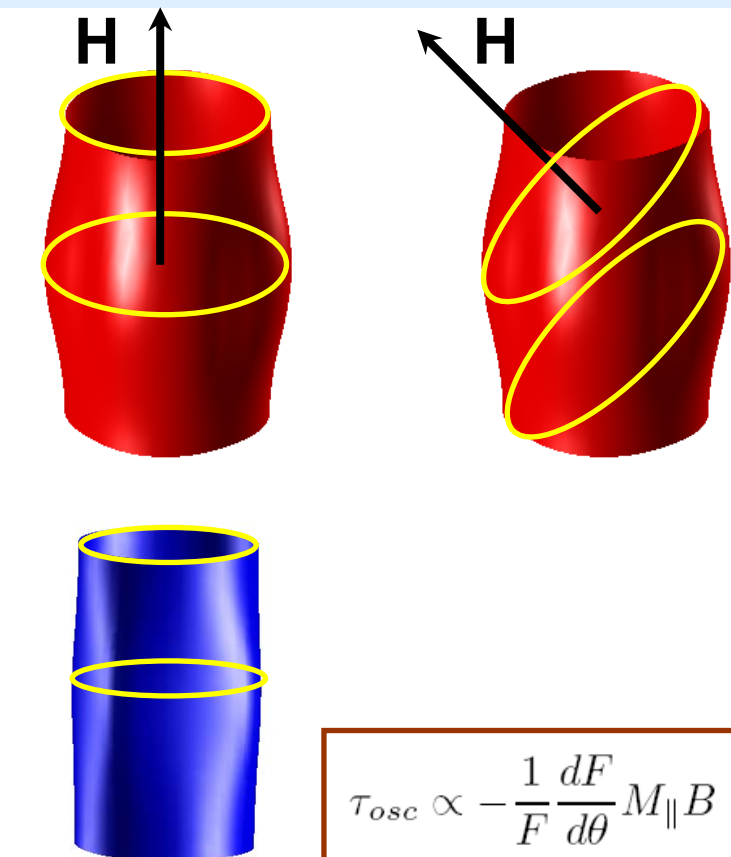
Fermi surface warping and Yamaji angle



$F(\theta) = F(0) / \cos \theta$
Quasi-two dimensional cylinder;

$$\Delta F_\alpha / F_\alpha \sim 4\%;$$

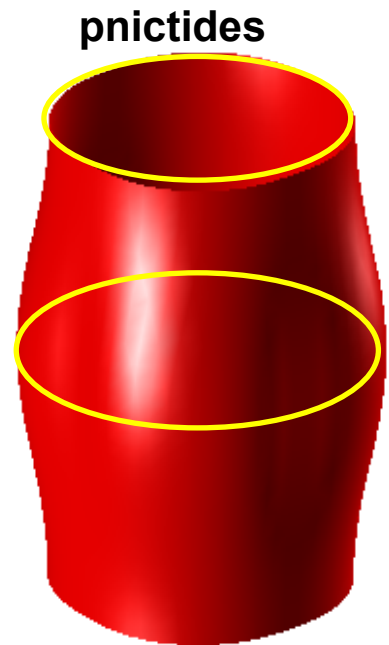
$$\Delta F_\beta / F_\beta \sim 23\%;$$



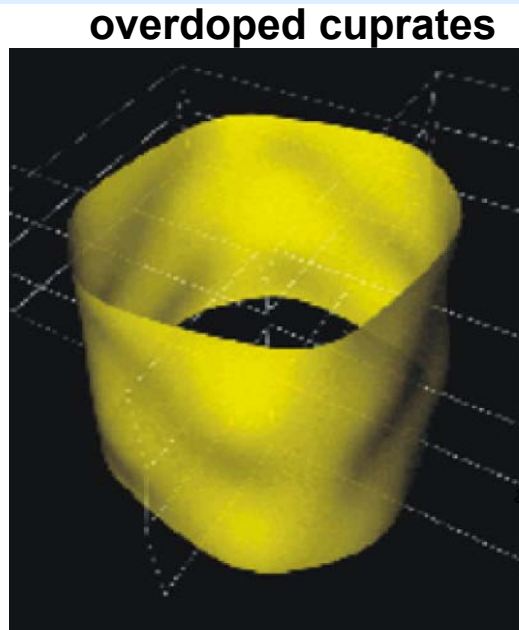
$$\tau_{osc} \propto -\frac{1}{F} \frac{dF}{d\theta} M_{||} B$$

At Yamaji angles all Fermi surface cross sections have equal areas; their magnetization contributions interfere constructively=peak effect.

Significant c-axis warping: of the Fermi surface 3D Fermi surfaces in 1111 compounds

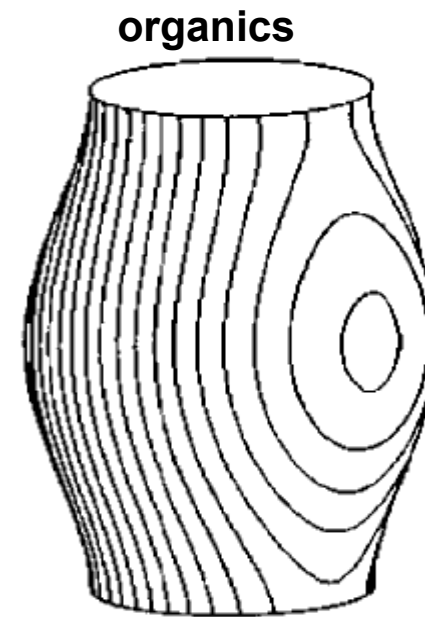


$\Delta F_\alpha/F_\alpha \sim 4\%$;
 $\Delta F_\beta/F_\beta \sim 23\%$;
 $\rho_c/\rho_{ab} \sim 10$



$Tl_2Ba_2CuO_{6+\delta}$

$\Delta F/F < 1\%$;
 $\rho_c/\rho_{ab} \sim 10^3$

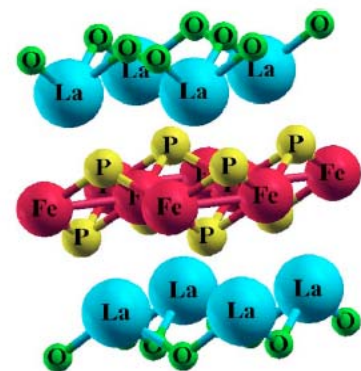


β -(BEDT-TTF)₂IBr₂

$\Delta F/F < 1.3\%$;
 $\rho_c/\rho_{ab} \sim 10^4$

$$\frac{2t_\perp}{\epsilon_F} = \frac{\Delta F}{2F}$$

Band structure of LaFePO: spaghetti



Conduction
FeP layer

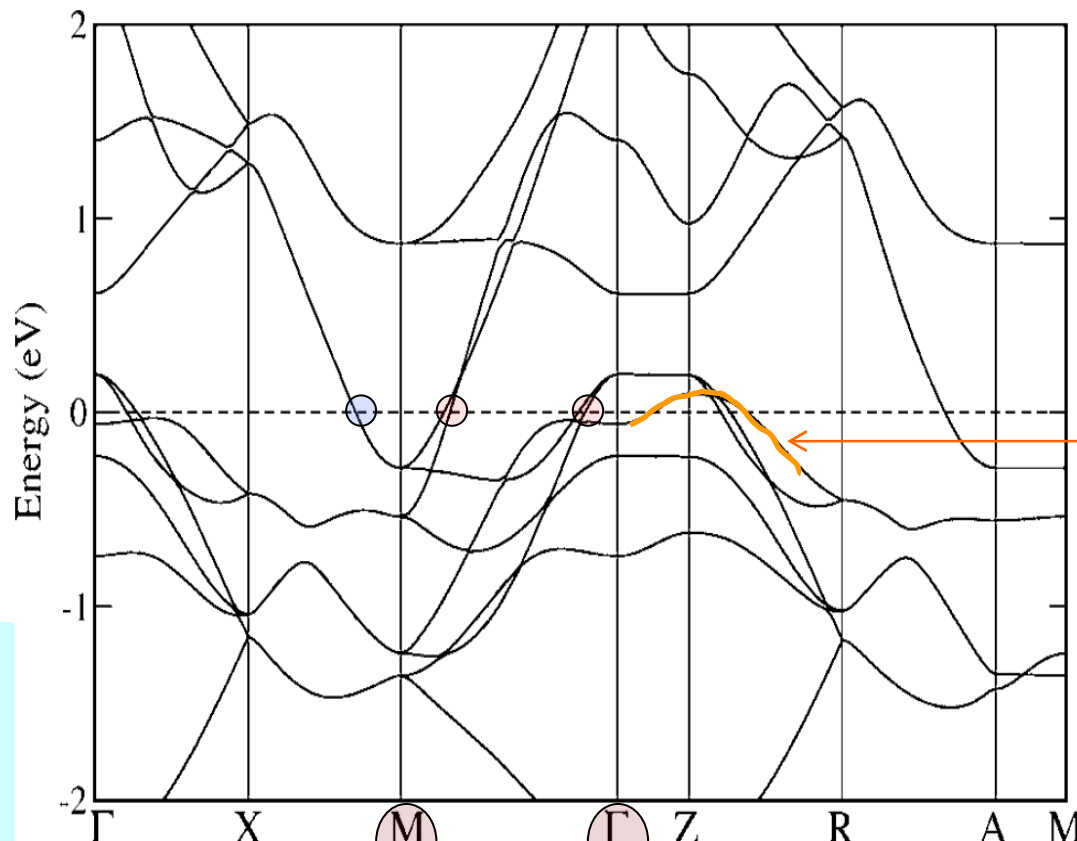
Electron pockets
centred at **M**
point: dxz , dyz



band 4



band 5

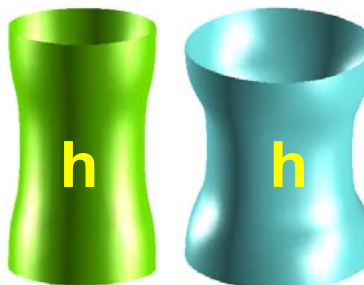


3D d_z^2 hole
pocket at Z most
susceptible to P
position and
doping;

band 1

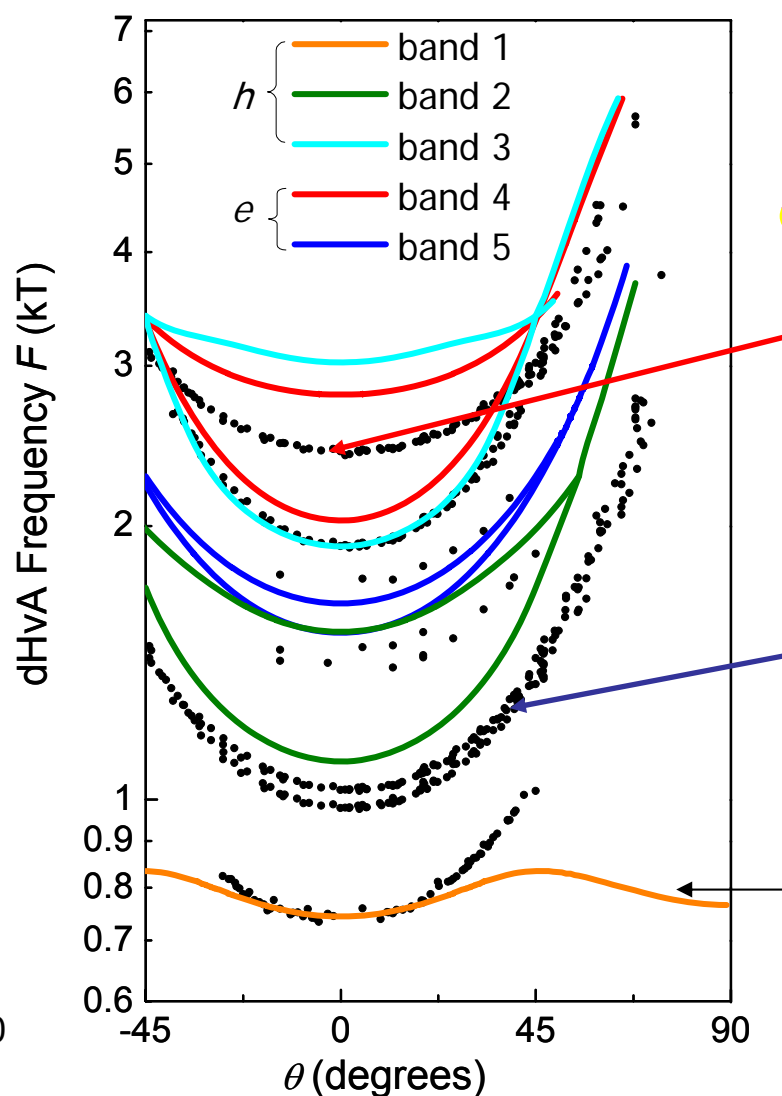
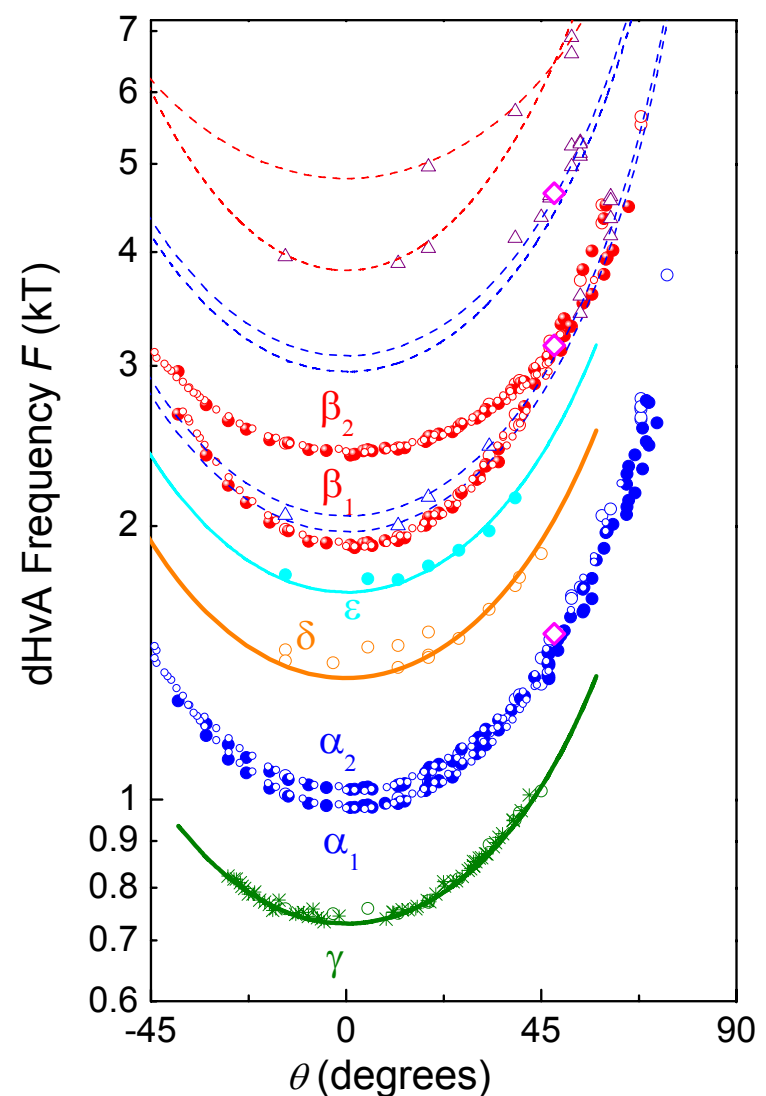


Hole pockets
centred at Γ
point: dxz, dyz



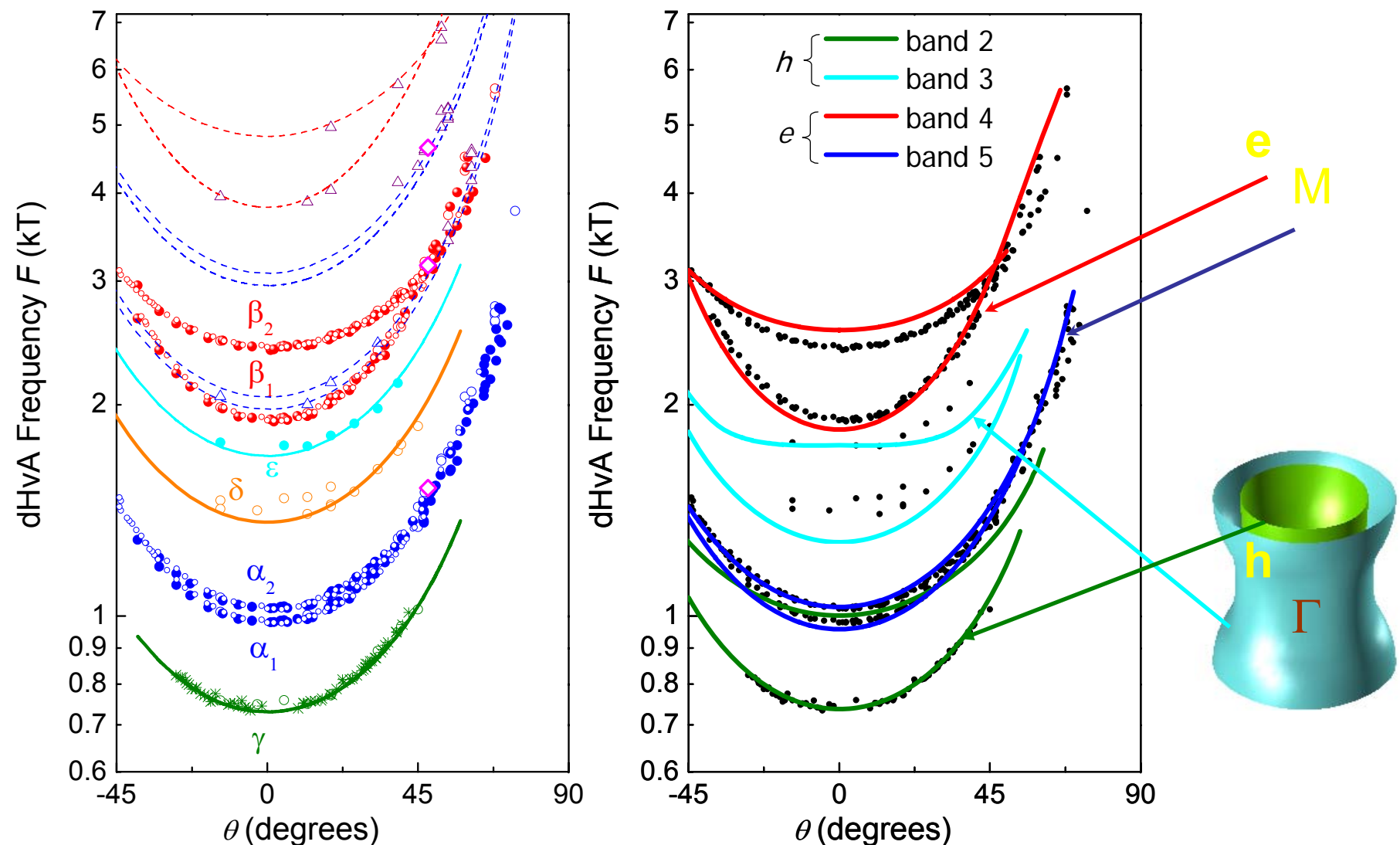
bands 2 and 3

dHvA data versus band structure calculations



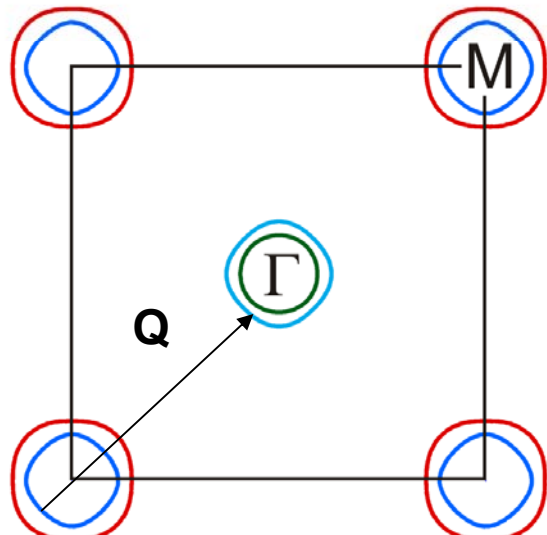
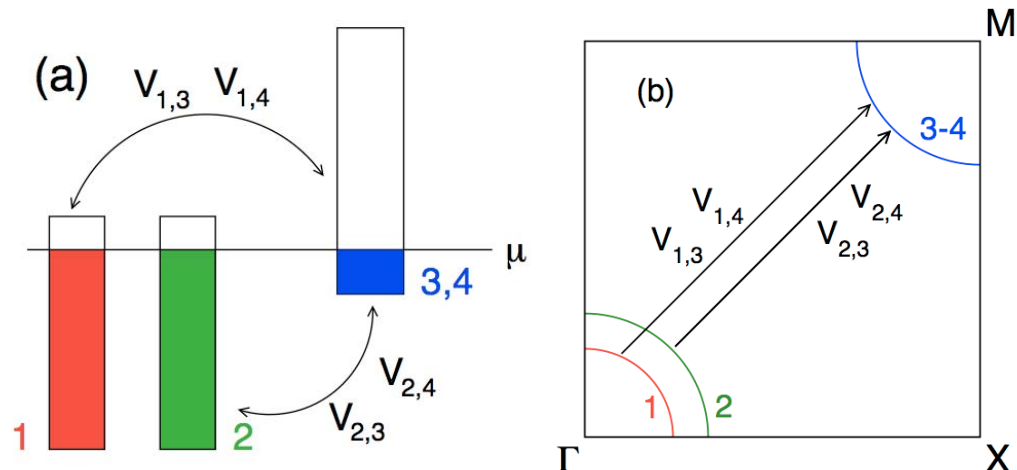
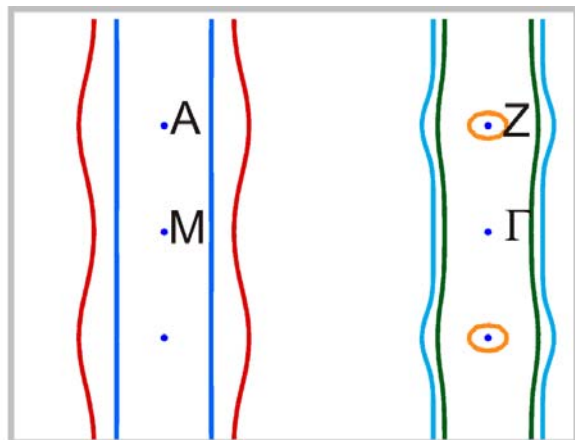
- electronic branches show similar dispersion to the experimental α and β pockets;
- no experimental branch matches the weak dispersion due to the 3D hole pocket;

Band shifting and charge balance



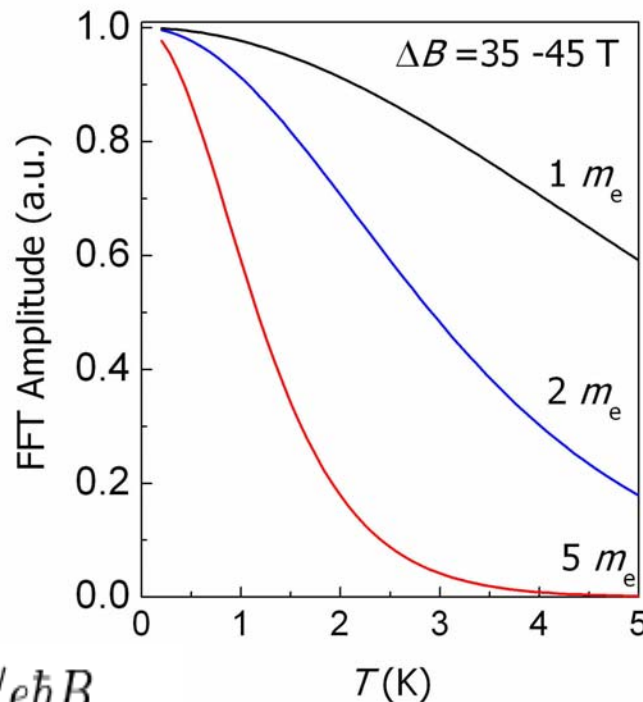
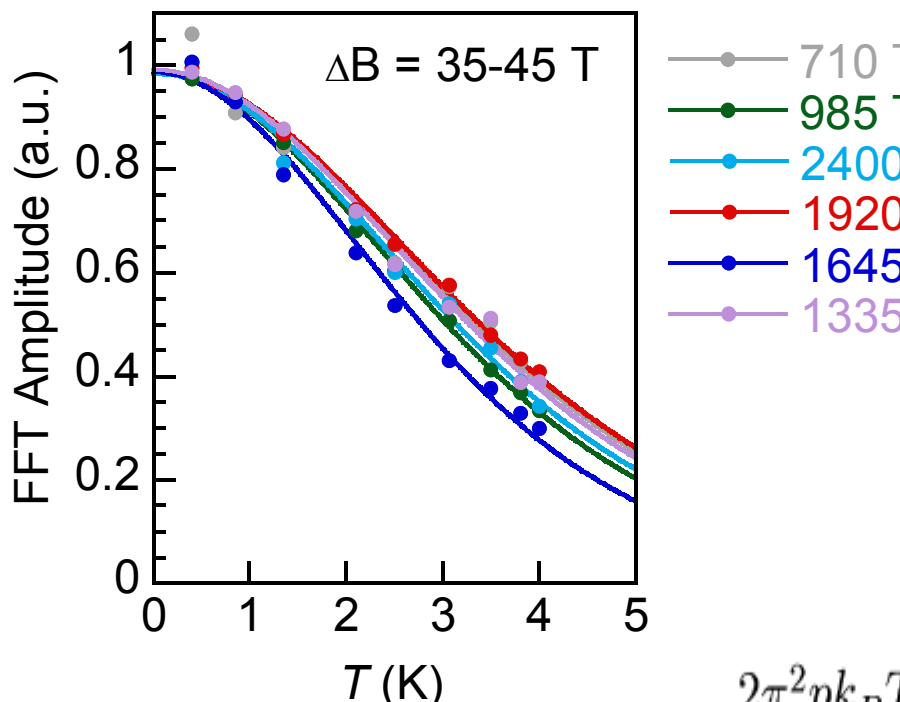
Electron bands shifted by $\Delta E = +85$ meV (band 5), $+30$ meV (band 4); hole bands all shifted by $\Delta E = -53$ meV; Charge imbalance ~ 0.034 el/fu; $\sim 1.7\%$ oxygen deficiency in LaFePO.

Shrinking of the Fermi surface in LaFePO



experimental observation of upward shift of the electron bands and of a downward shift of the hole band may be evidence of dominance of interband scattering (nesting);

Moderate mass enhancement in LaFePO



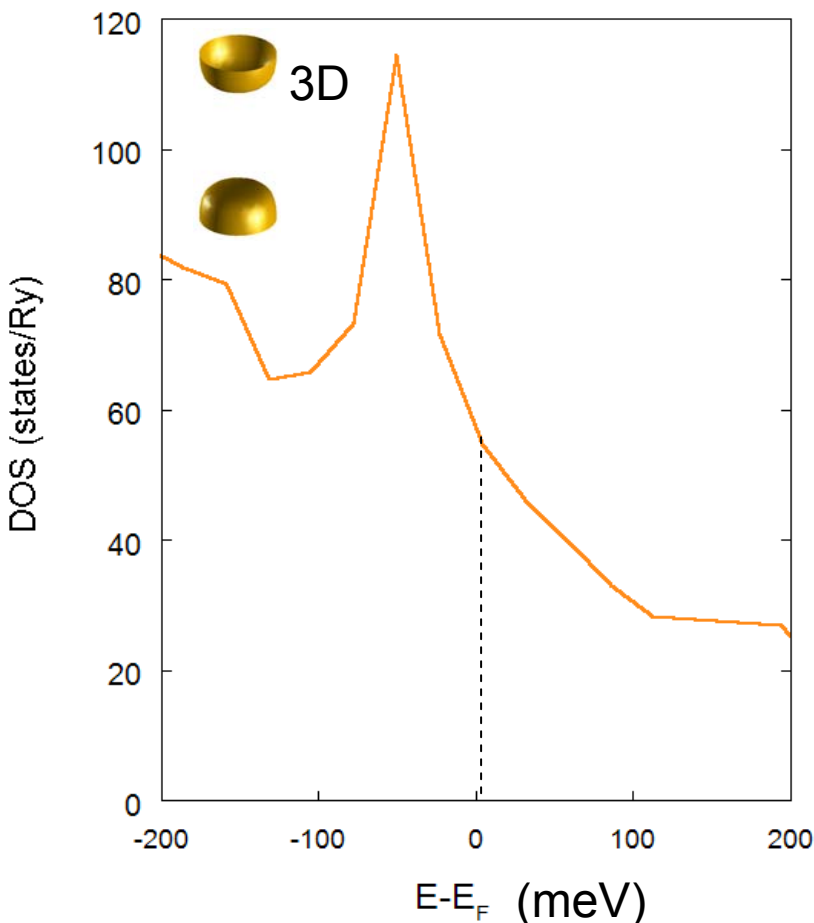
$$R_T = \frac{2\pi^2 p k_B T m^*/e\hbar B}{\sinh(2\pi^2 p k_B T m^*/e\hbar B)}$$

$m^*/m_b = (1 + \lambda) \approx 2.$

(el-el + el-ph)

- the effective masses between $1.7-2.1 m_e$ for both electrons and holes;
- moderate mass enhancement for the electronic bands;

Electronic contribution to the specific heat



E_F lies just above a peak in the DOS, which leads to a rapidly decreasing DOS with energy.

$$\frac{C}{T} = \frac{\pi k_B^2 N_A a^2}{3\hbar^2} \times \sum m_i^*$$

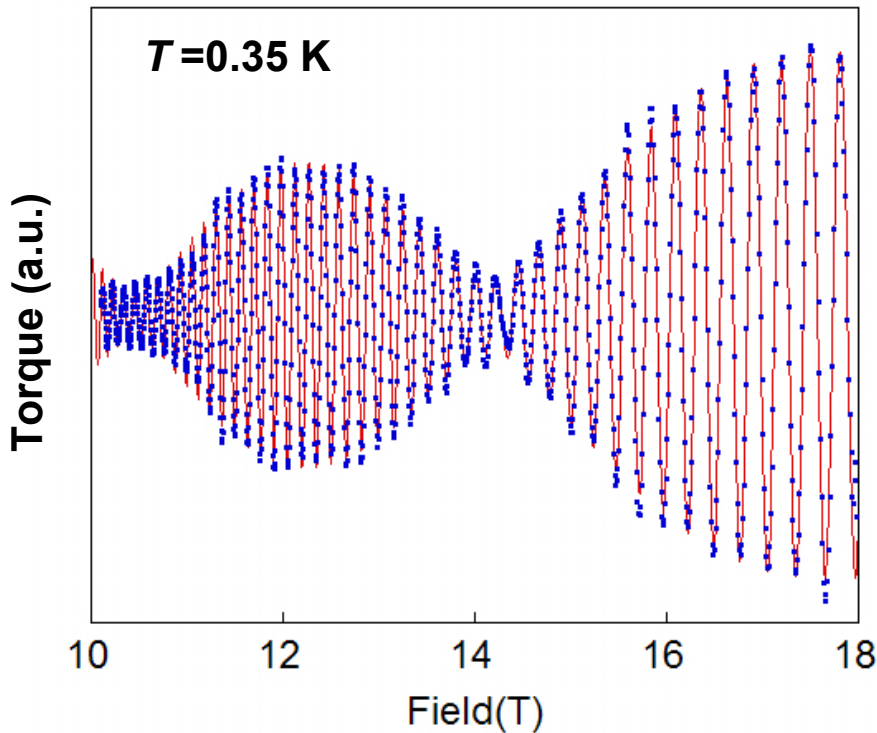
$\gamma_{\text{exp_powder}} \sim 7 - 12 \text{ mJ/mol K}^2$;

$\gamma_{\text{dHvA}} = 6 \text{ mJ/mol K}^2$;

Assuming 4 quasi-two dimensional cylinders with $m^* \sim 2 m_e$;

3D pocket absent?

Quasiparticle scattering rates in LaFePO



$$R_D = \exp(-\pi k_F/eB\ell)$$

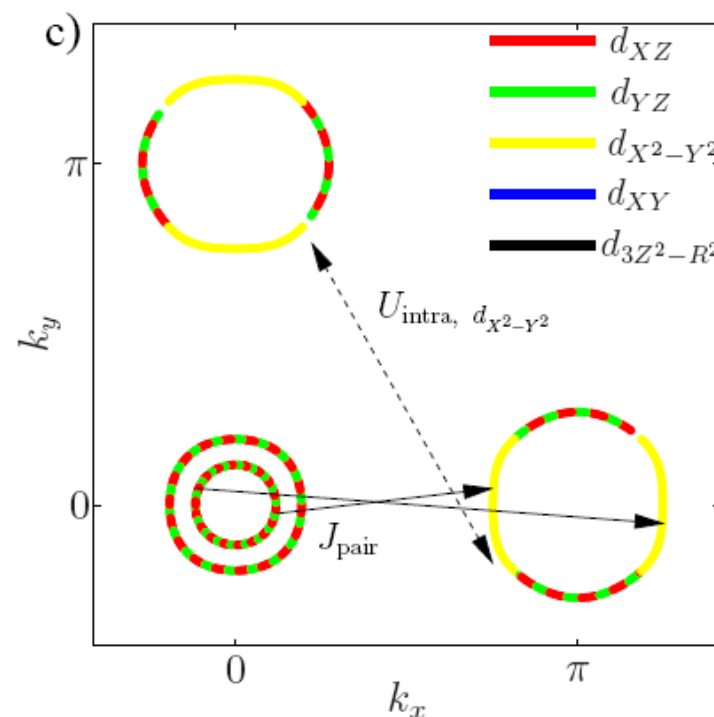
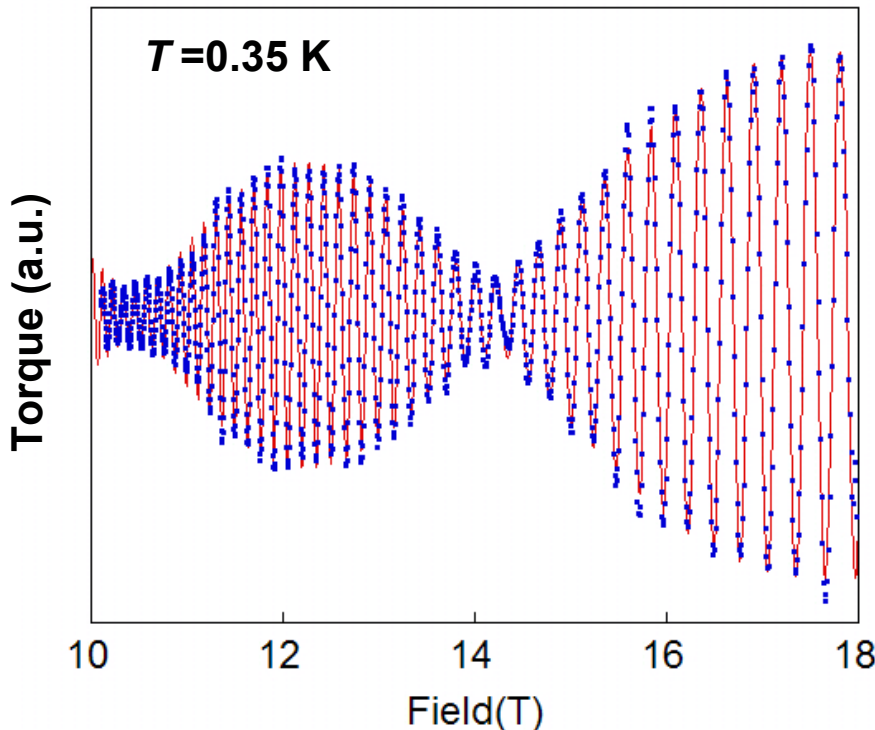
k_F is the orbitally averaged Fermi wavevector for the particular Fermi surface orbit;

$$l_\alpha \sim 1300 \text{ \AA}$$

inelastic quasiparticle mean free-path
(small and large angle scattering from impurities)

- mean free path: electrons $l_\alpha \sim 1300 \text{ \AA}$ and $l_\beta \sim 800 \text{ \AA}$; scattering for **hole** ~ factor 2 larger;

Relevance of the orbital character of bands



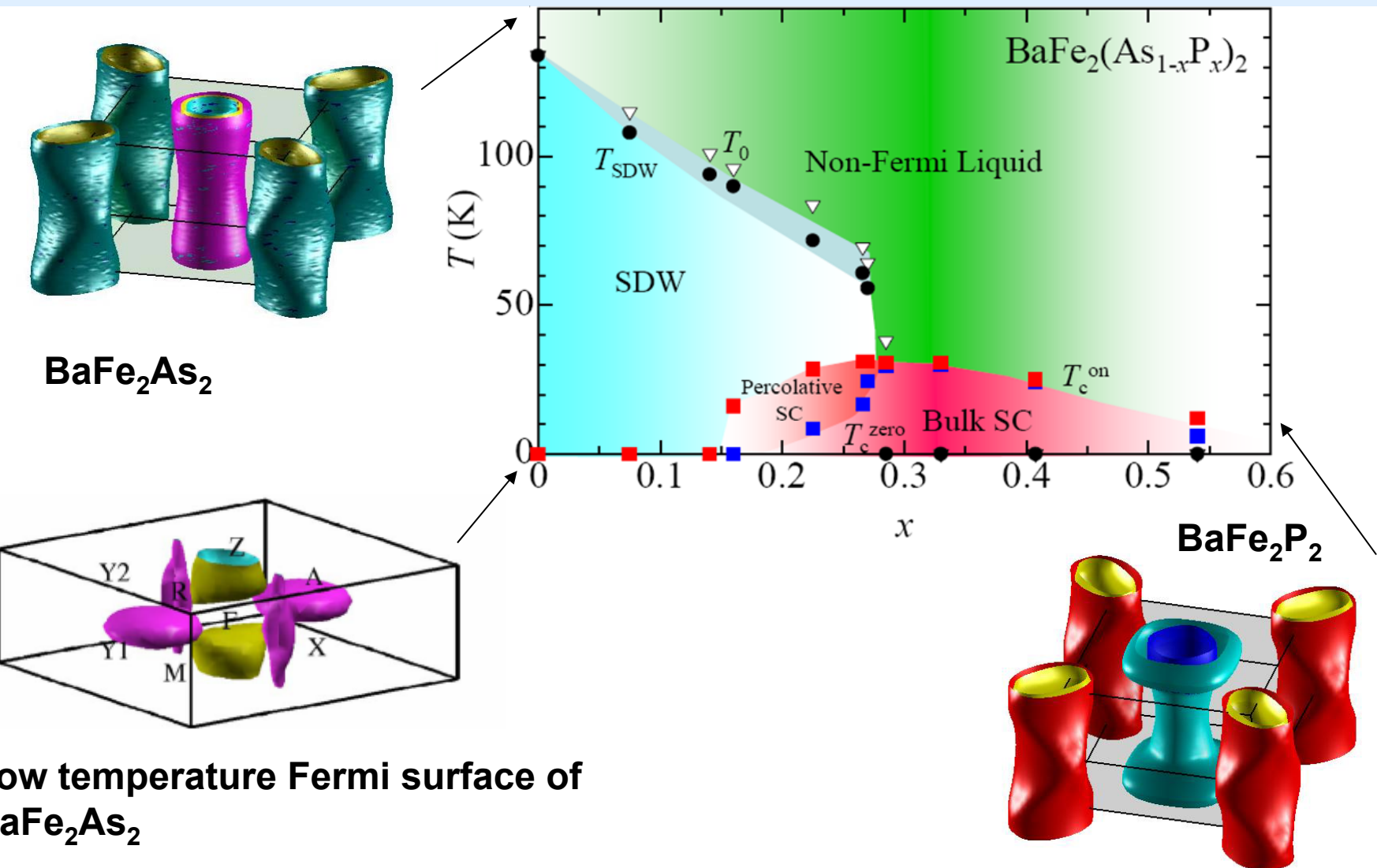
$$R_D = \exp(-\pi k_F/eB\ell)$$

k_F is the orbitally averaged Fermi wavevector for the particular Fermi surface orbit;

$I_\alpha \sim 1300 \text{ \AA}$
inelastic quasiparticle mean free-path
(small and large angle scattering from impurities)

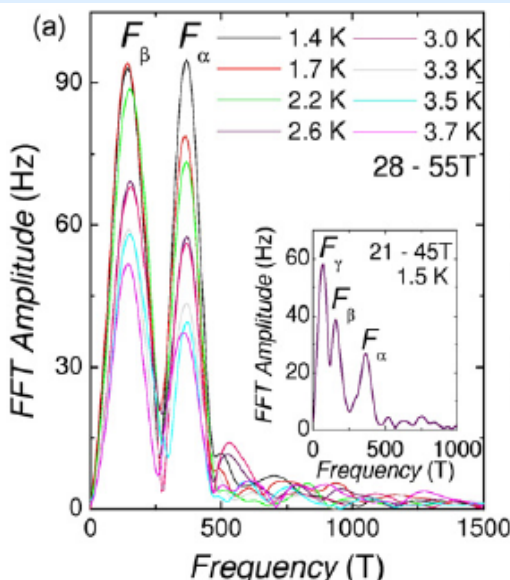
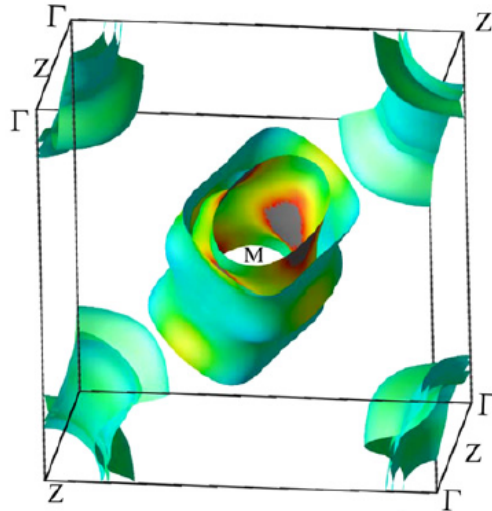
- mean free path: electrons $I_\alpha \sim 1300 \text{ \AA}$ and $I_\beta \sim 800 \text{ \AA}$; scattering for hole ~ factor 2 larger;

Effect of chemical pressure: P substitution



Reconstructed Fermi surface in the AFM phase

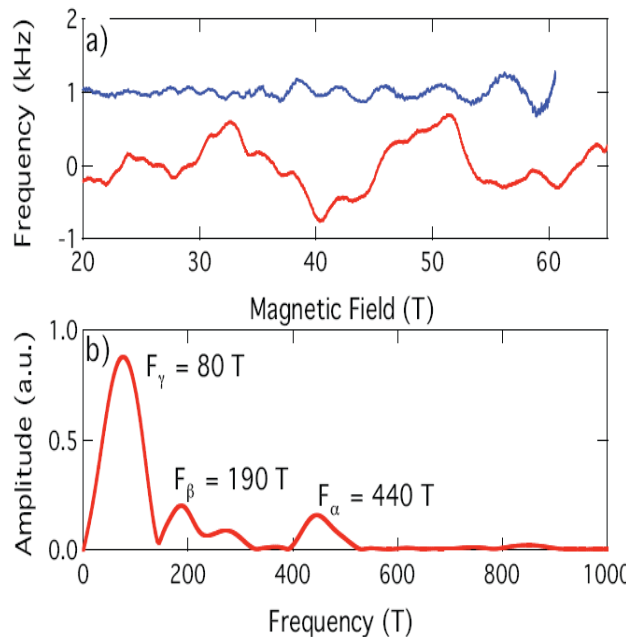
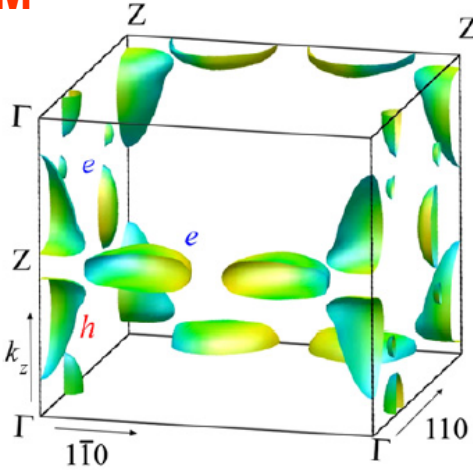
PM



SrFe₂As₂

S. Sebastian *et al.*,
J. Phys.: Cond. Mat. 20 (2008) 422203

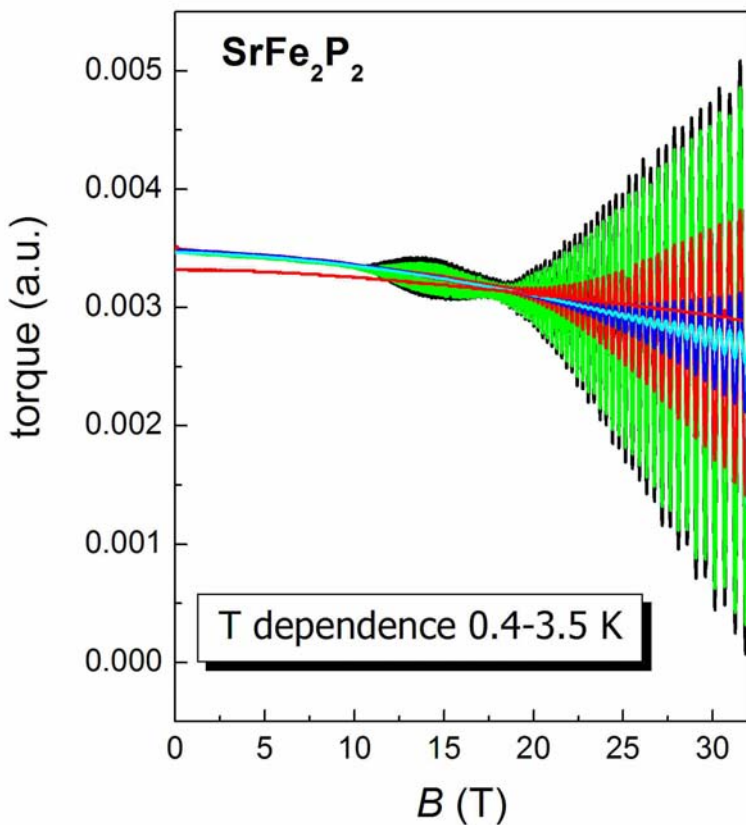
AFM



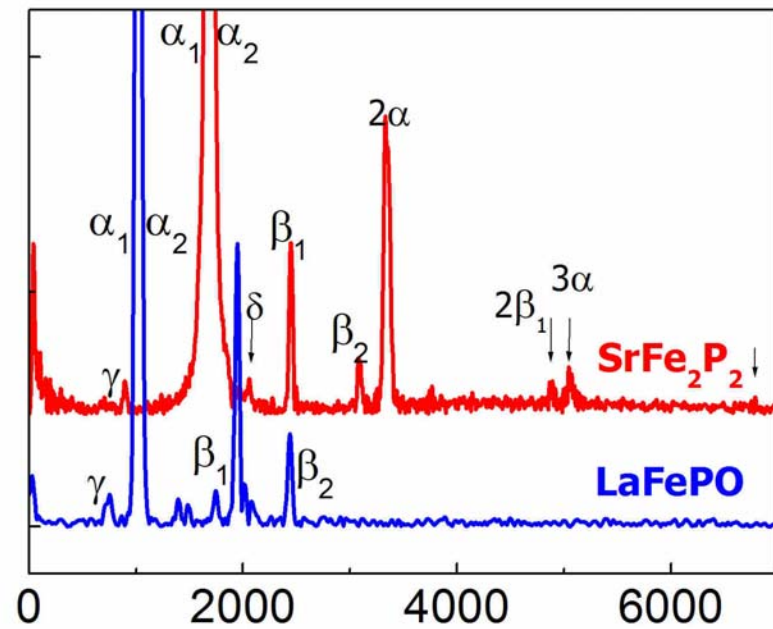
BaFe₂As₂

J. Analytis *et al.*,
arXiv: 0902.1172 (2009)

Quantum oscillations in SrFe_2P_2

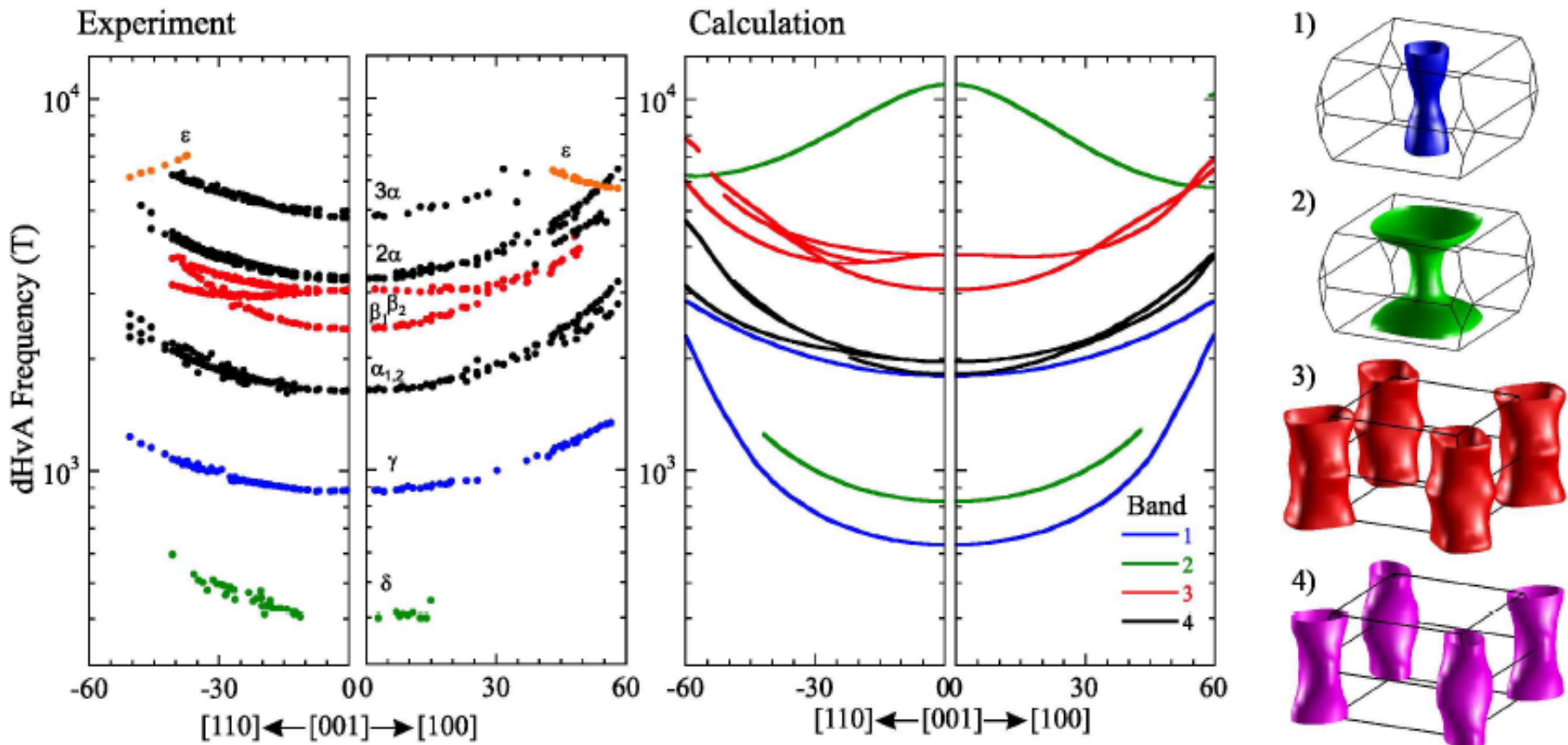


SrFe_2P_2 is non-magnetic and non-superconducting with bond angle **116.34°** (away from a perfect tetrahedron with **109.47**)



Electronic bands α and β shows the largest amplitude; the least affected by scattering (if masses the same);

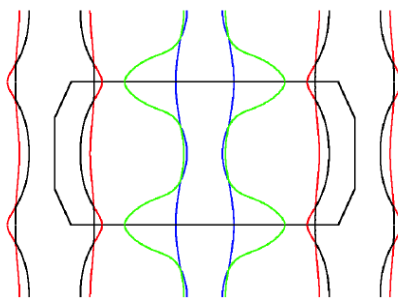
Fermi surface of SrFe_2P_2



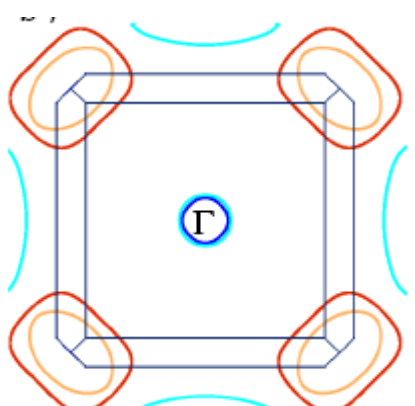
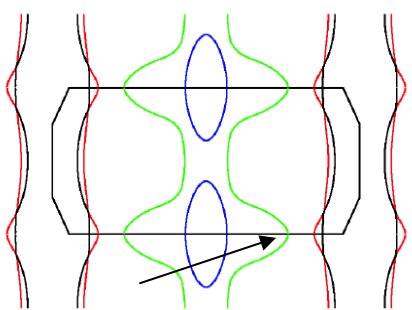
Electronic bands in very good agreement with band structure calculations; band shifts still needed. Nesting?

Fermi surface of SrFe_2P_2

Not Shifted



Shifted



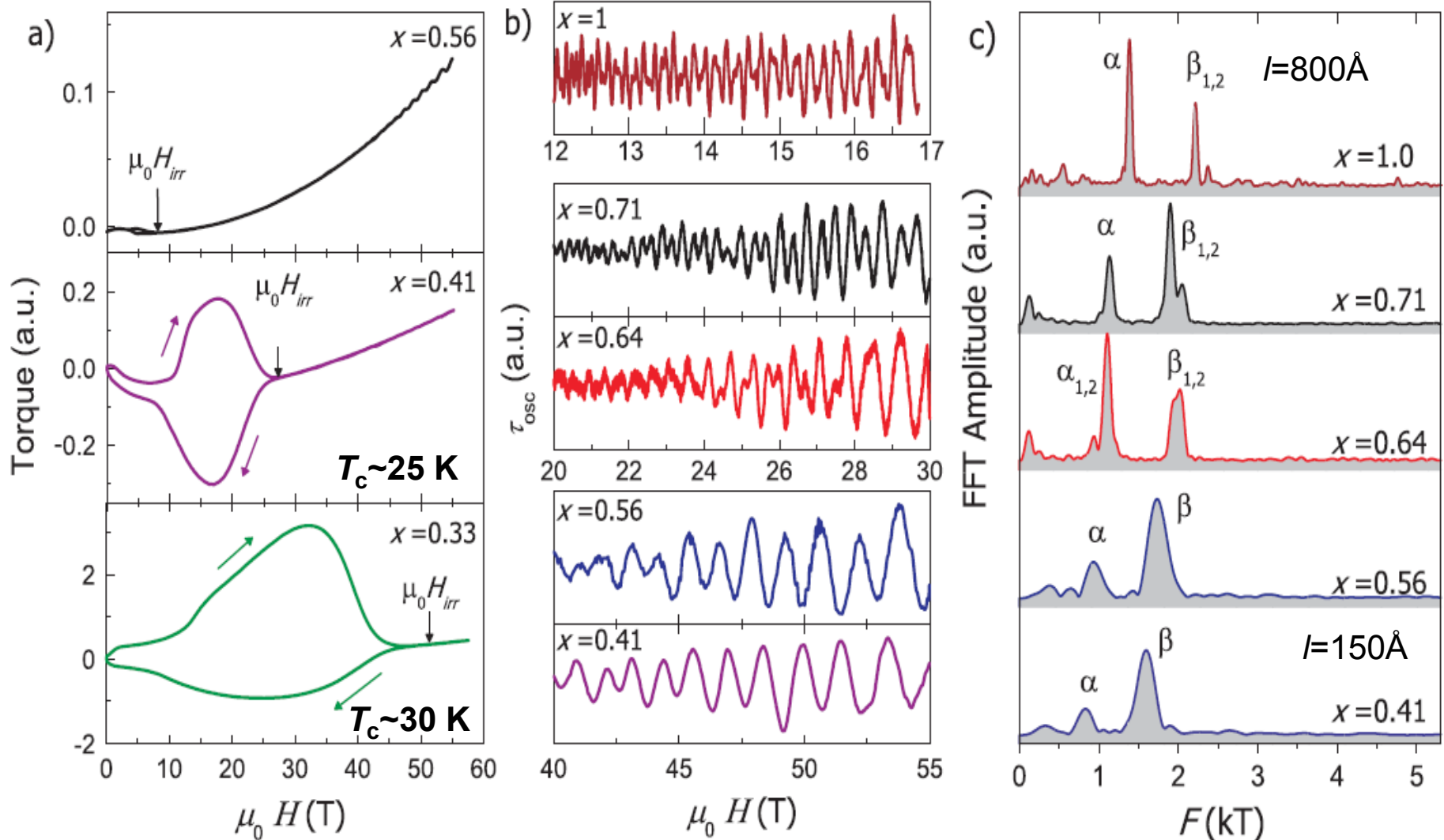
holes

electrons

	Experiment			Calculations			
	$F(\text{kT})$	$\frac{m^*}{m_e}$	$\ell(\text{nm})$	Orbit	$F(\text{kT})$	$\frac{m_b}{m_e}$	$\frac{m^*}{m_b}$
					1_{\min}	0.632	0.97
γ	0.89	1.49(2)	58	1_{\max}	1.804	1.07	1.4
δ	0.41	1.6(1)	21	2_{\min}	0.828	1.24	1.3
ϵ	6.02*	3.41(5)*	90	2_{\max}	10.95	2.30	1.7
β_1	2.41	1.92(2)	63	3_{\min}	3.077	1.25	1.6
β_2	3.06	2.41(3)	70	3_{\max}	3.824	1.70	1.6
α_1	1.637	1.13(1)	100	4_{\min}	1.823	0.55	2.1
α_2	1.671	1.13(1)	100	4_{\max}	1.966	0.60	2.1

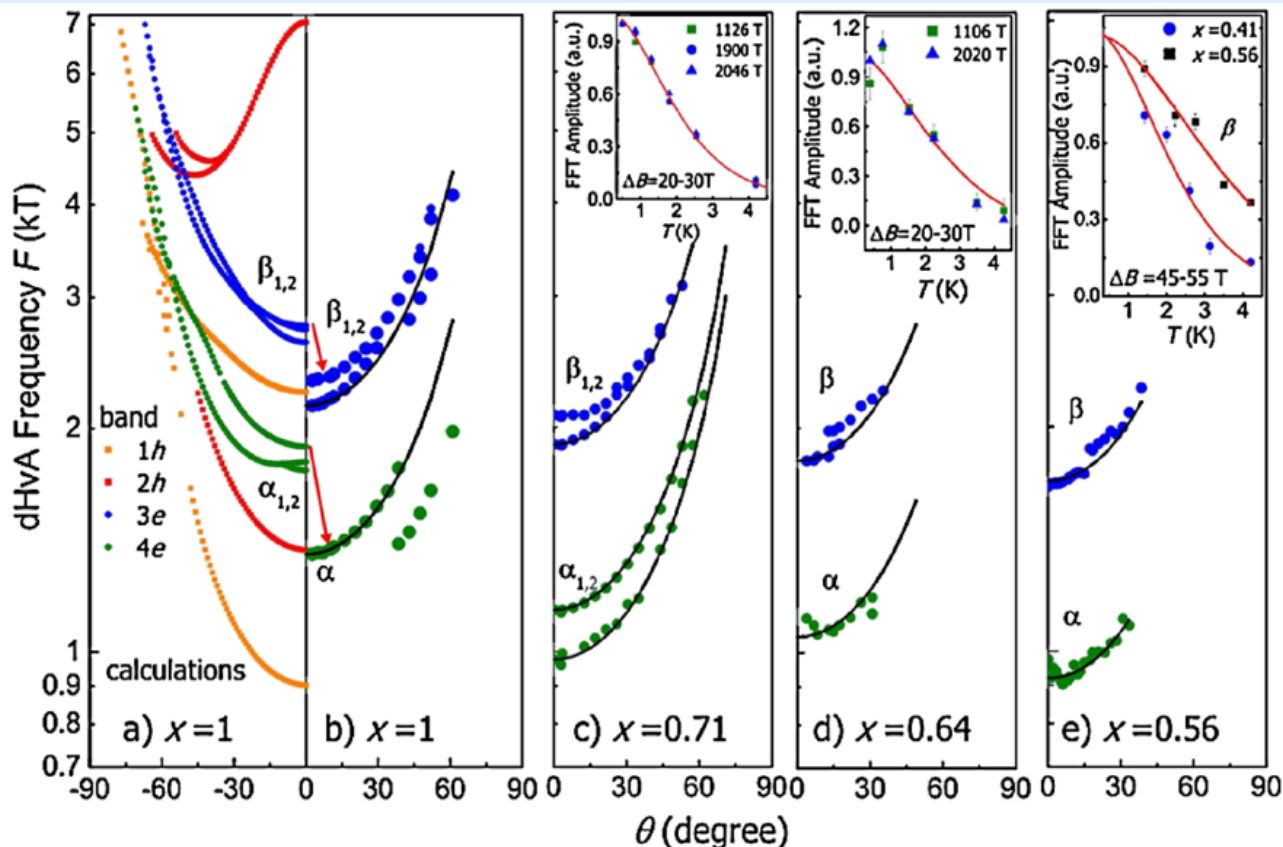
- Moderate mass enhancement sheet dependent and anisotropy in scattering;
- Nesting strongly diminished-strongly warped cylinders and a three-dimensional hole pocket; some nesting may be possible along k_z ;

Evolution of Fermi surface in $\text{BaFe}_2(\text{As}_{1-x}\text{P}_x)_2$



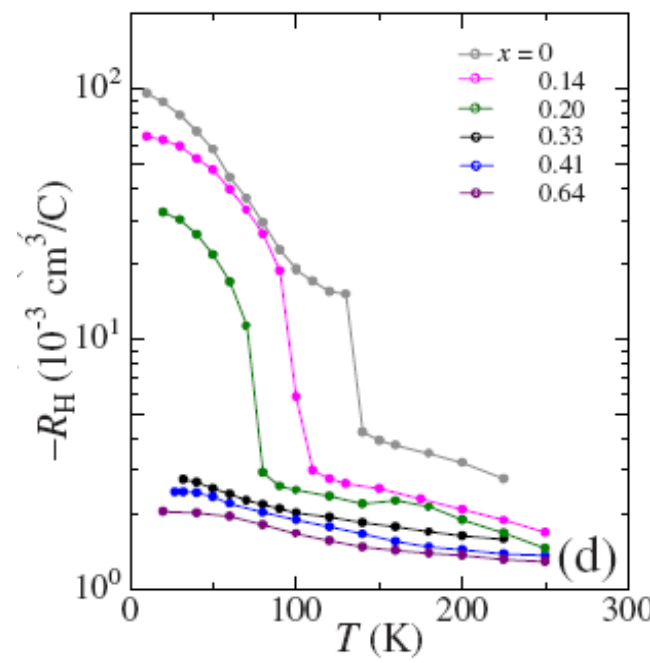
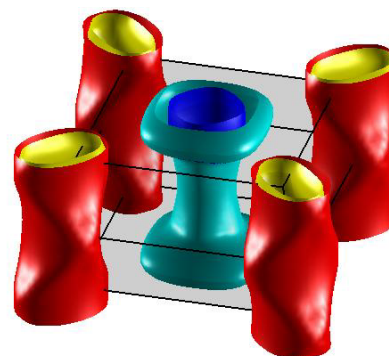
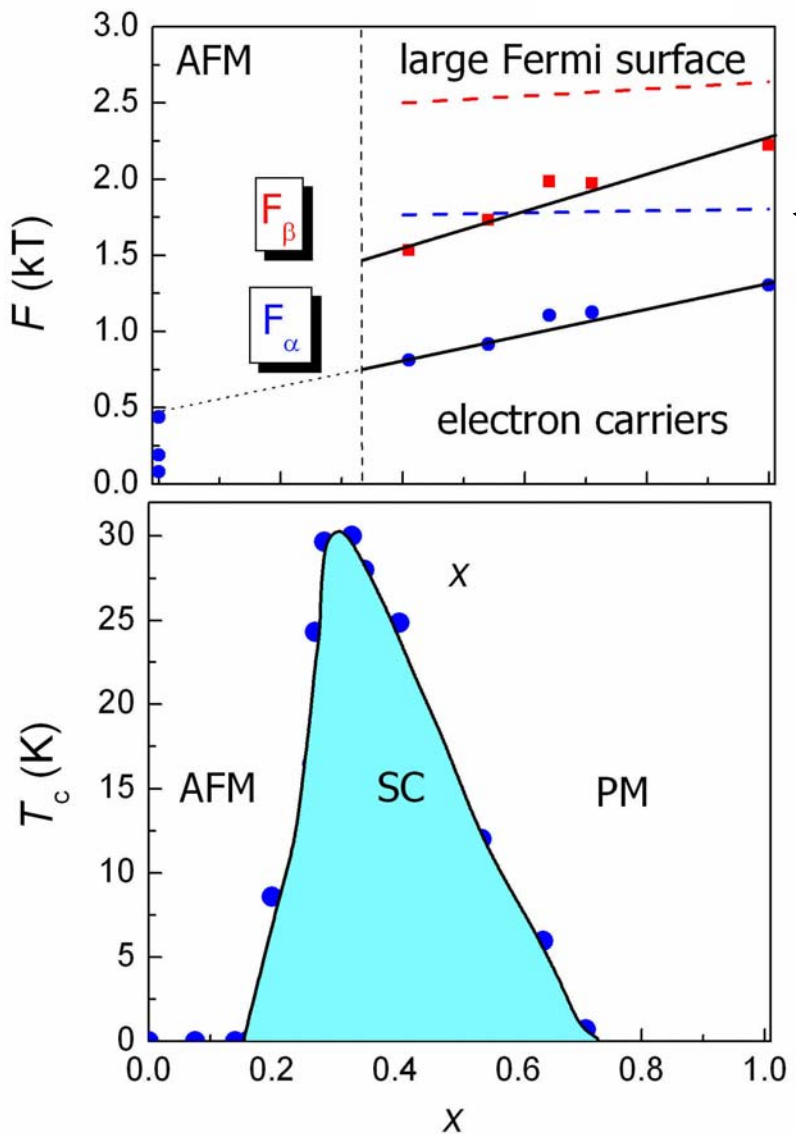
oscillations observed for materials with $T_c = 0 - 25$ K; $T_{\max} = 30$ K for $x = 0.33$;

Evolution of electronic pockets in $\text{BaFe}_2(\text{As}_{1-x}\text{P}_x)_2$

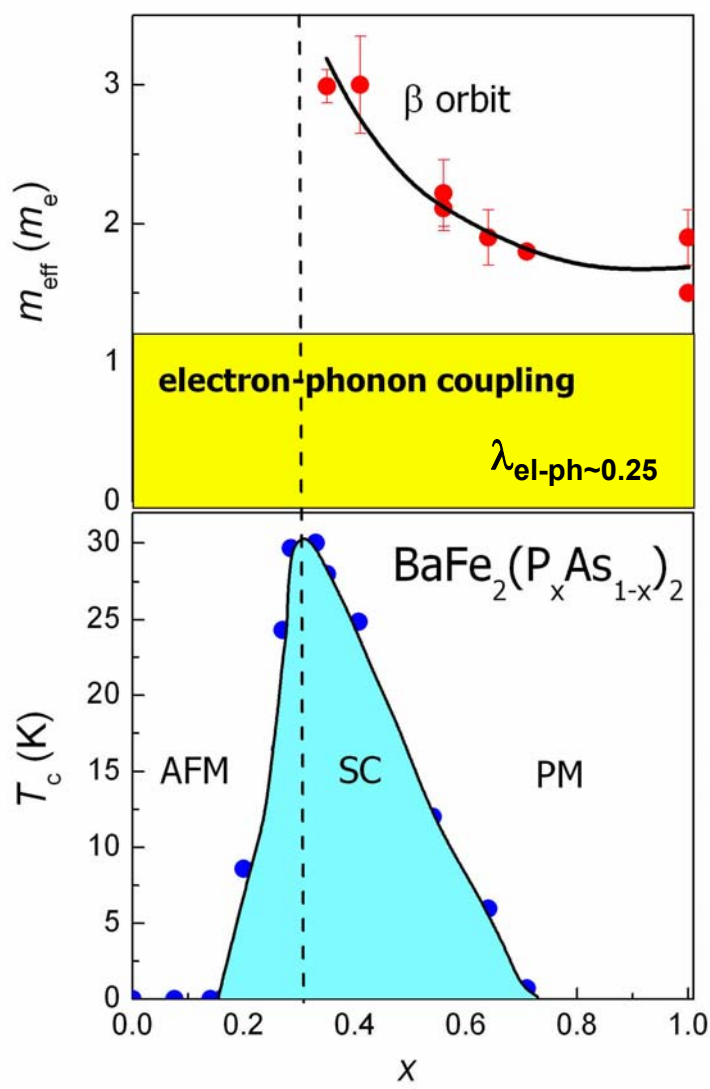


- Two electron cylindrical Fermi surfaces;
- Volume: Decrease with decreasing x (no doping);

Fermi surface shrinking in $\text{BaFe}_2(\text{As}_{1-x}\text{P}_x)_2$

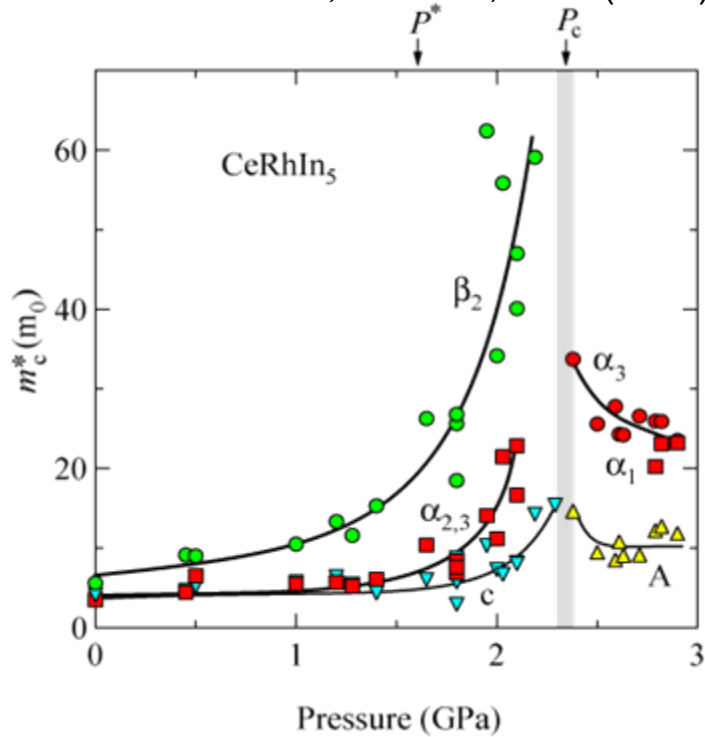


Enhancement of the effective mass in $\text{BaFe}_2(\text{As}_{1-x}\text{P}_x)_2$



$\gamma_{\text{expr}} \sim 18 \text{ mJ/mol K}^2$ ($x=0.38$); (arXiv:1002.3355)

H. Shisido *et al.*, JPSJ 74, 1103 (2005)

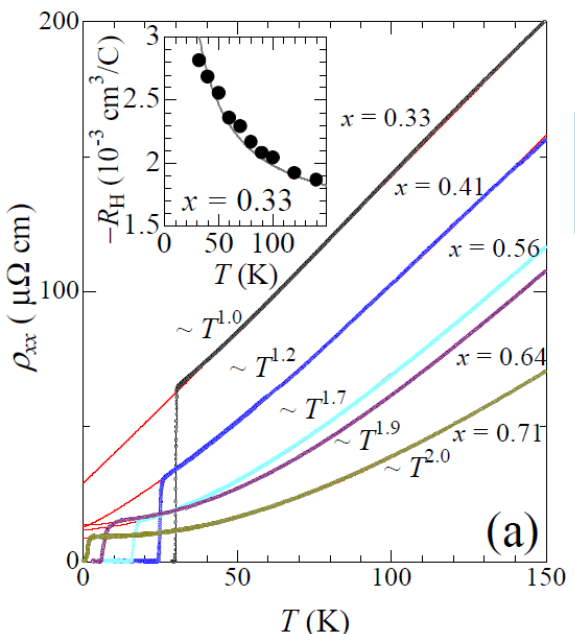
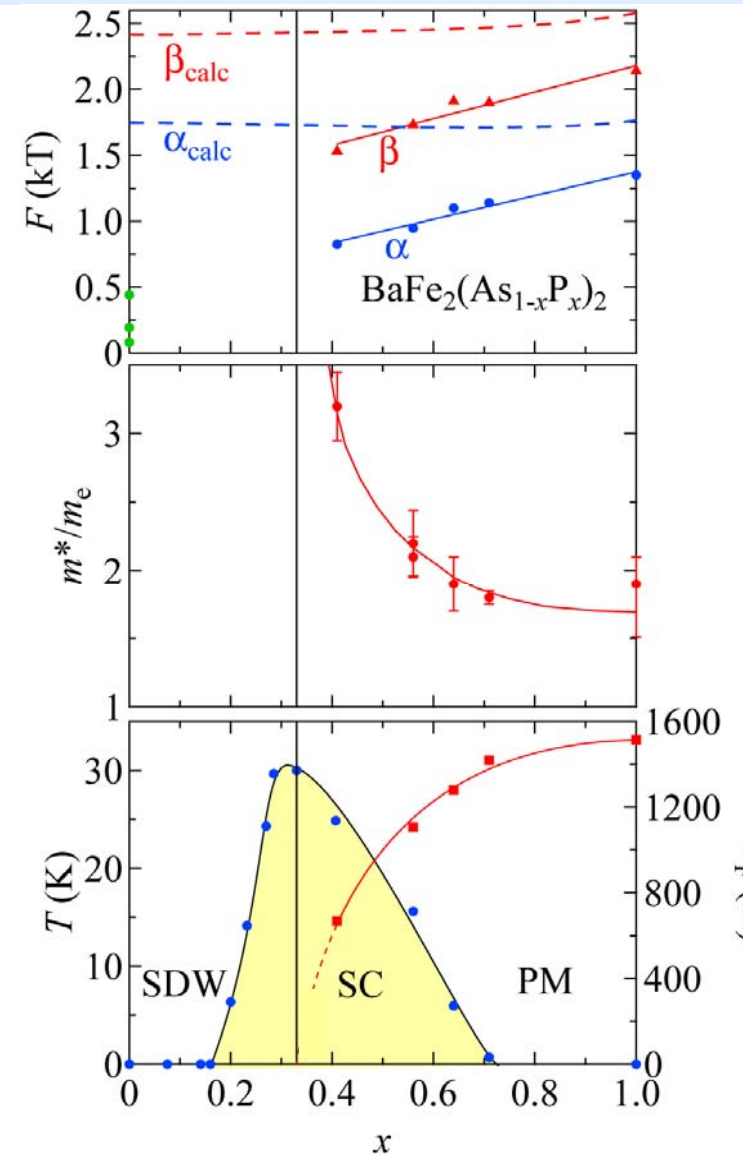


Increase of effective mass due to many-body interactions; Decrease of T_F

$$T_F = \frac{\hbar e F}{m^* k_B}$$

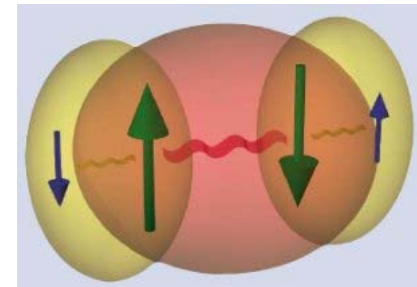
Quantum critical behavior ?

Spin fluctuations in $\text{BaFe}_2(\text{As}_{1-x}\text{P}_x)_2$

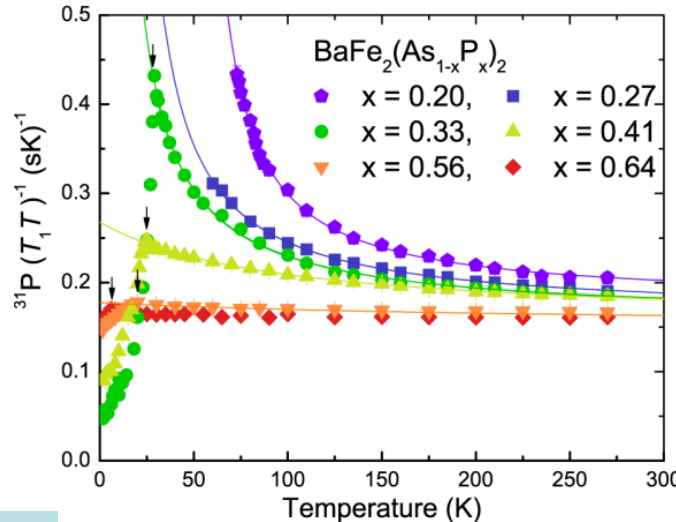


$$\rho = \rho_0 + AT^\alpha$$

S. Kasahara et al.,
PRB 81, 184519 (2010)



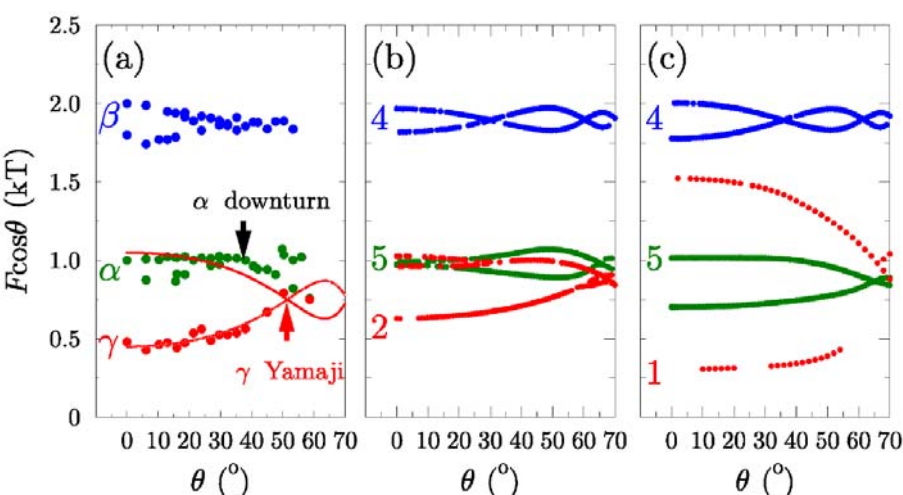
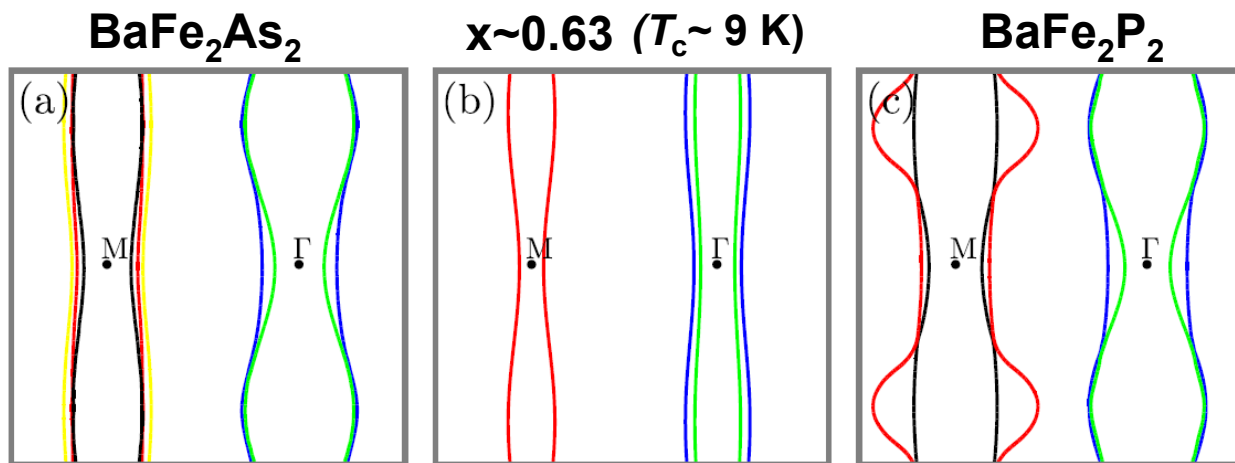
Antiferromagnetic spin fluctuations close to QCP



$$1/T_1 T \sim 1/(T+\theta)$$

Y. Nakai, et al.
arXiv:1005.2853
(2010)

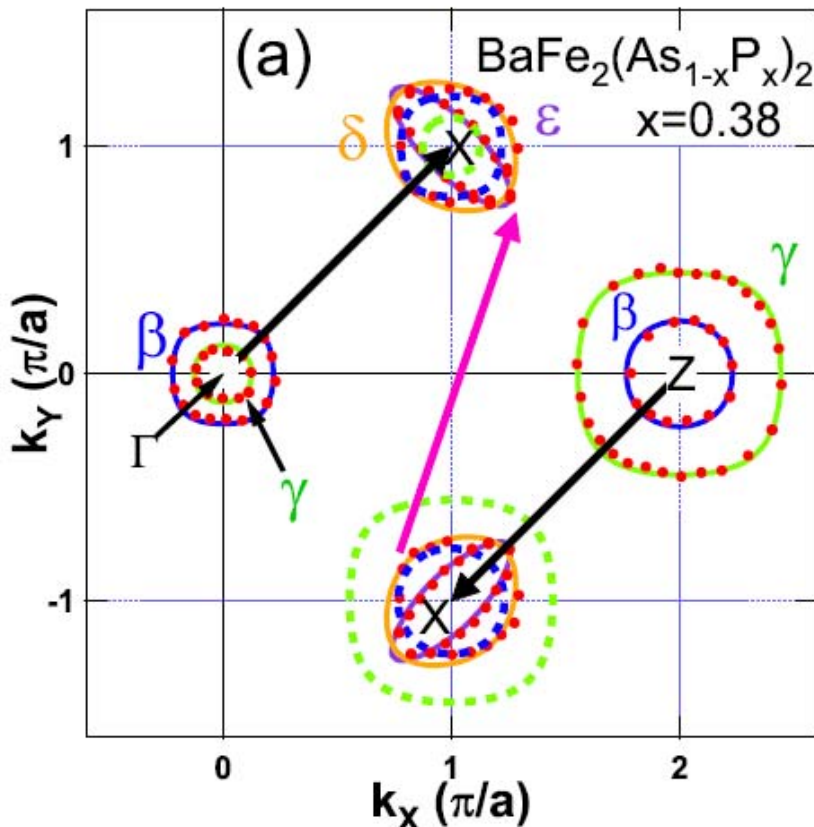
Enhanced nesting towards maximum T_c ?



	Experiment			Calculations			
	F(kT)	$\frac{m^*}{m_e}$	$\ell(\text{nm})$	Orbit	F(kT)	$\frac{m_b}{m_e}$	$\frac{m^*}{m_b}$
γ	0.45	4.5(5)	12	2 _{min}	.53	1.24	3.6
				2 _{max}	0.86	1.72	
α_1	.89	2.3(1)	-	5 _{min}	1.02	1.25	1.8
α_2	1.10	2.10(5)	48	5 _{max}	1.04	1.31	1.6
β_1	1.80	2.1(1)	-	4 _{min}	1.81	1.17	1.8
β_2	2.01	2.0(5)	57	4 _{max}	1.95	1.30	1.5

- One further HEAVY hole pocket observed; inner electron pocket and inner hole pocket have similar sizes ; shrinking of the electronic bands;

ARPES studies in $\text{BaFe}_2(\text{As}_{1-x}\text{P}_x)_2$ ($x=0.38$)

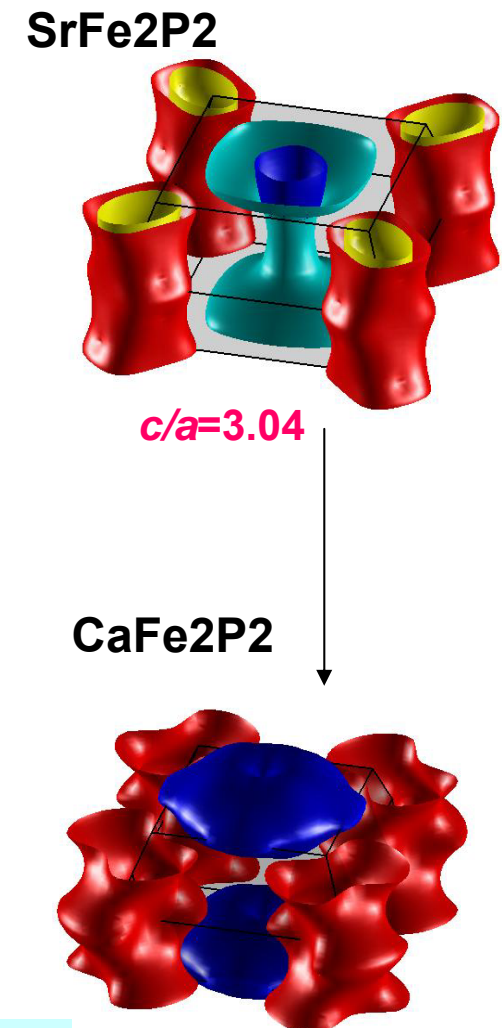
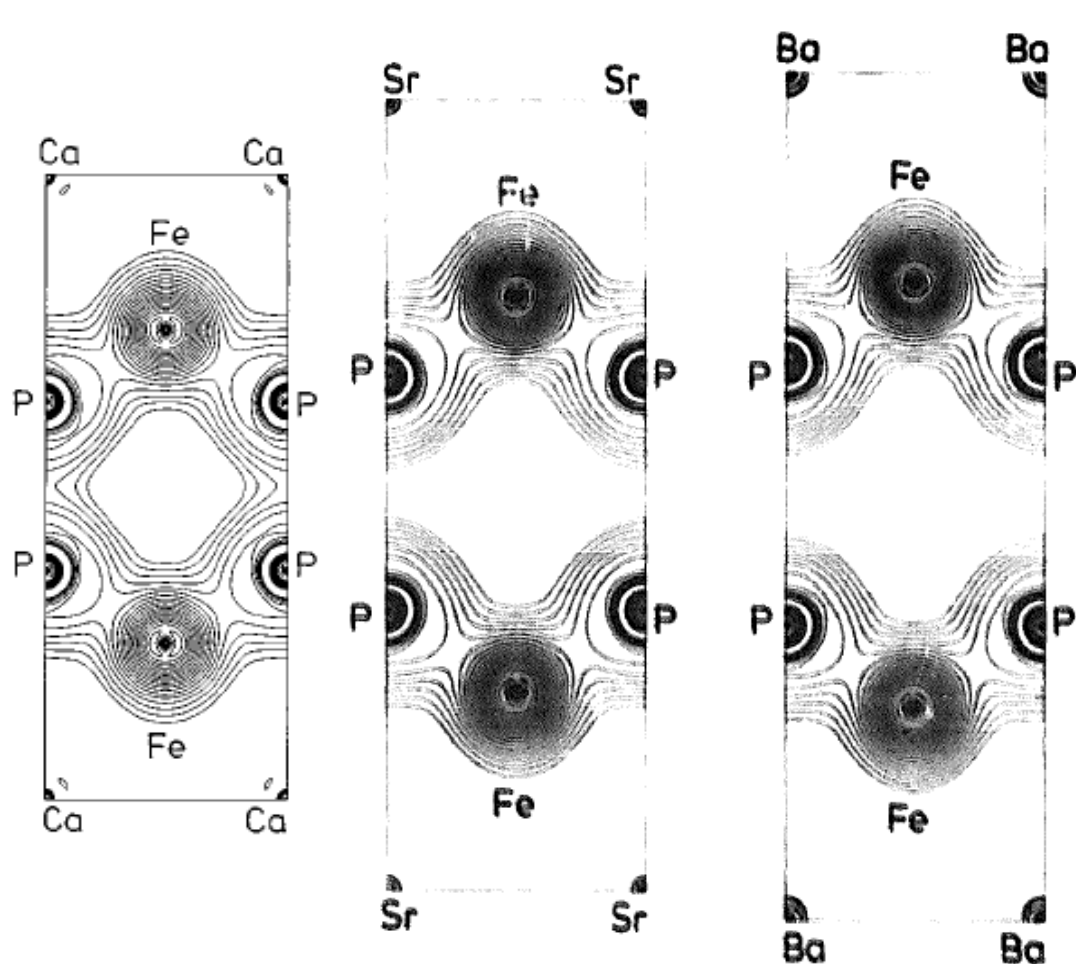


	FS	3D volume	k_z	2D area	m^*/m_e	m_b/m_e	m^*/m_b
β h	3.9	Γ	3.9	3.8	1.3	2.9	
		Z	3.8	2.5	1.2	2.1	
γ h	6.0	Γ	1.0	2.6	0.9	2.9	
		Z	16.3	3.9	2.3	1.7	
δ e	5.3	X	5.3	2.8	0.71	3.9	
ϵ e	3.4	X	3.0	2.0	0.93	2.1	

Mass enhancement for all orbits varies between 2 - 3.9

- one quasi-two dimensional electron and hole pockets have similar size and shape implying good nesting but they have different orbital character ($d_{xz/yz}$ for hole and d_{xy} for the electron sheet) so weak contribution to the spin susceptibility;

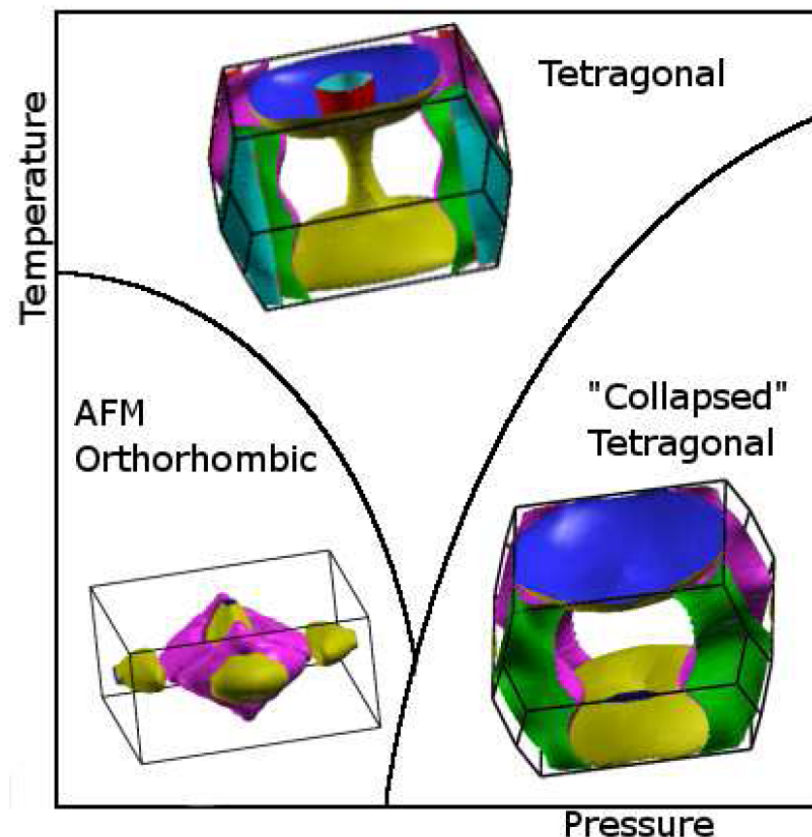
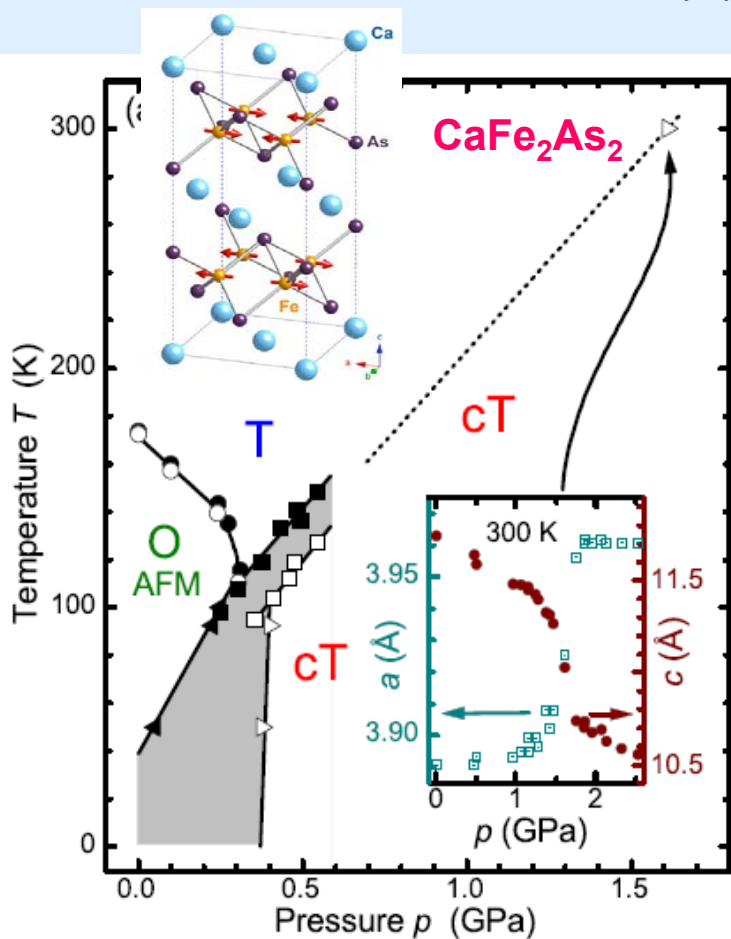
Significant pnictogen bonding affects FS



Small spacer between Fe layers enhances P-P bonding.

$c/a=2.65$

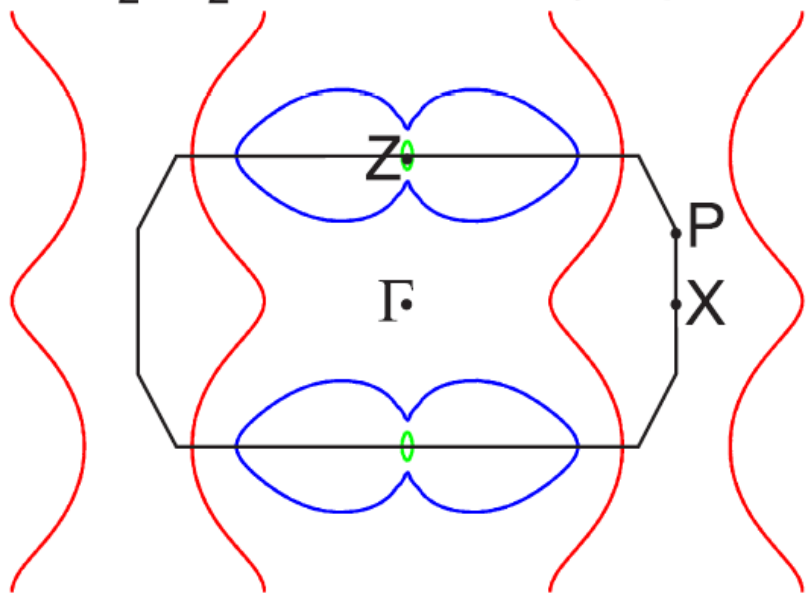
Effect of applied pressure in pcnitides



CaFe_2As_2 under pressure has a transition to a non-magnetic collapsed tetragonal (cT) state; ~ 10% decrease in the c -axis and a ~2% increase in the a -axis; $c/a=3$ in the tetragonal phase to $c/a=2.65$ in the cT phase;
• Superconductivity present under non-hydrostatic conditions (uniaxial pressure);

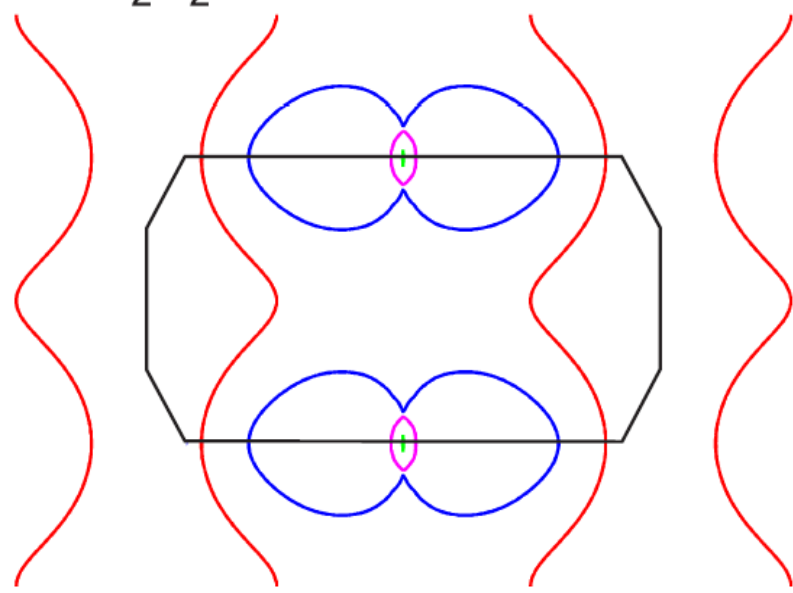
Effect of chemical pressure: small c/a ratio

CaFe_2As_2 P=0.63GPa (cT phase)



$c/a=2.65$

CaFe_2P_2 P=0

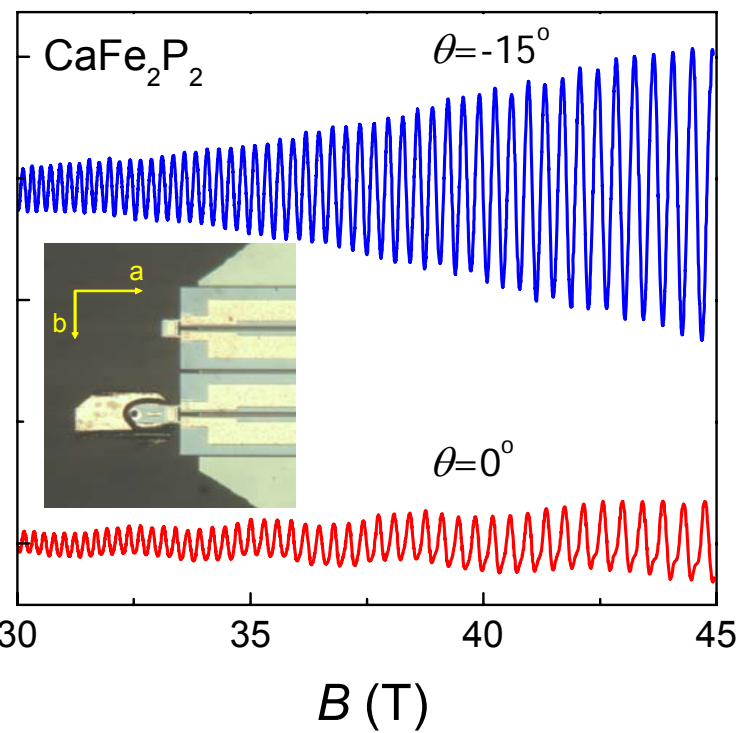


$c/a=2.59$

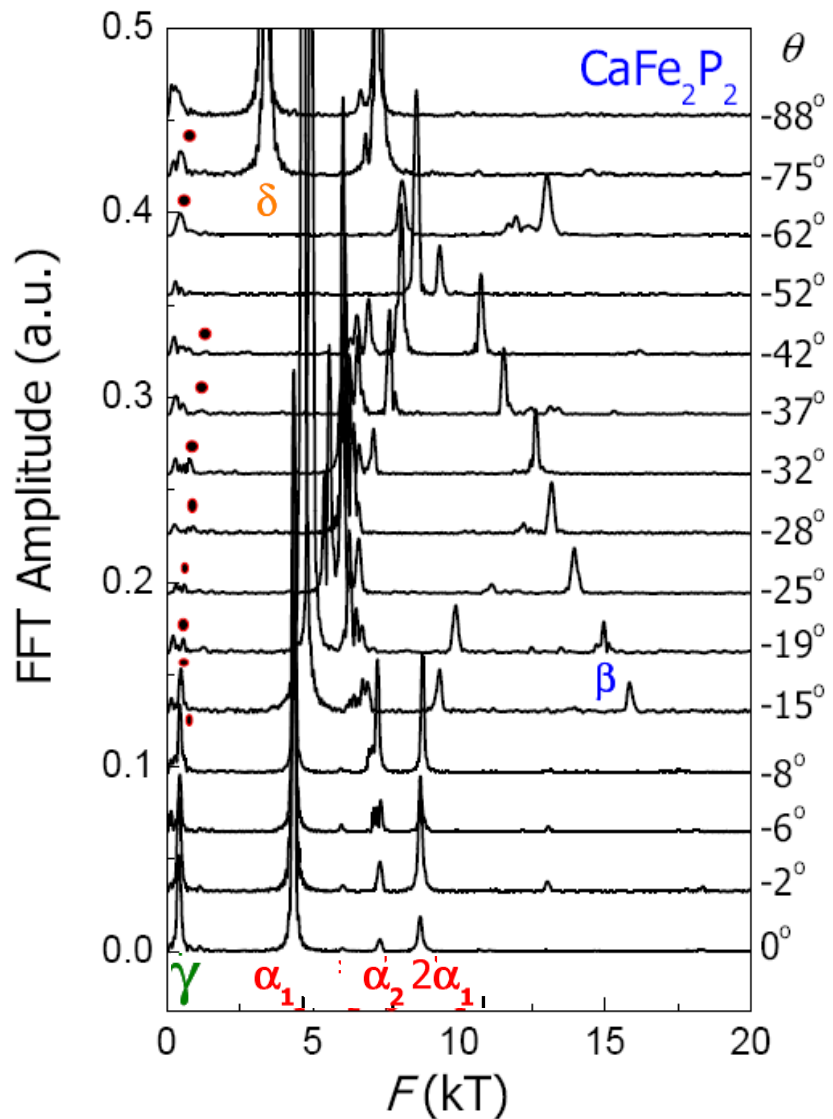
Band structure calculations predict:

- CaFe_2P_2 is a close structural analogue of the collapsed tetragonal non-magnetic phase of CaFe_2As_2 and shows a similar Fermi surface;
- single electron and hole sheets highly three-dimensional in character ;

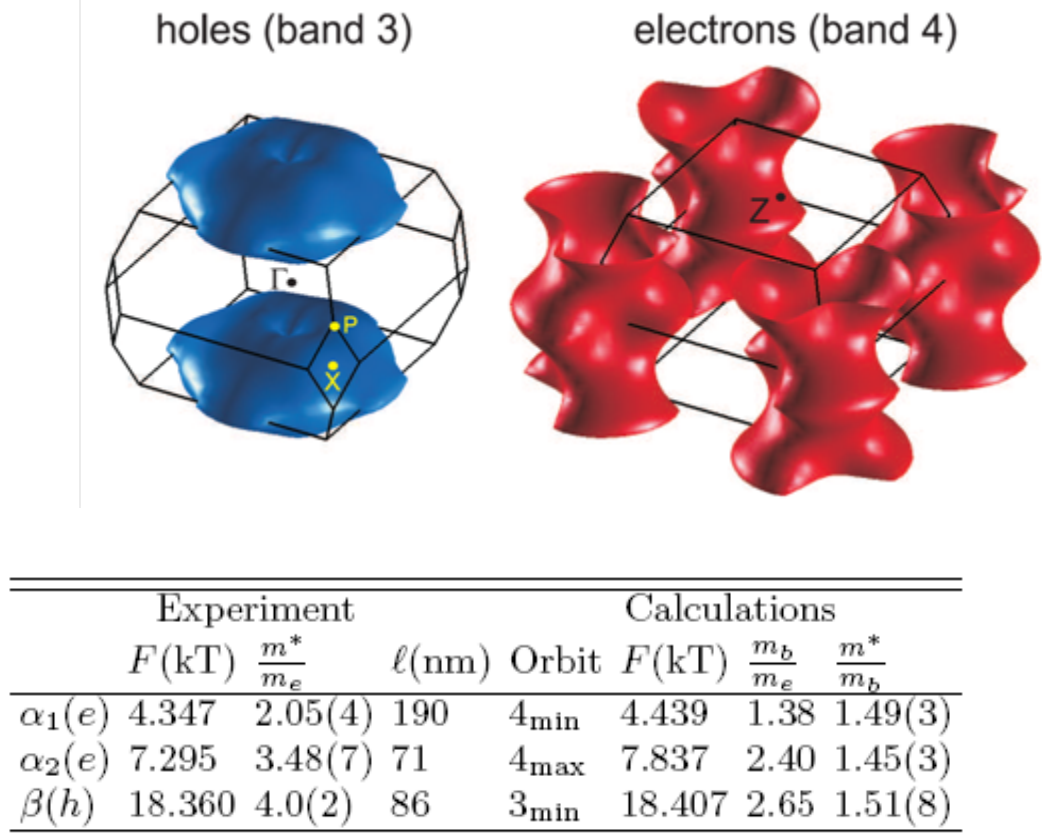
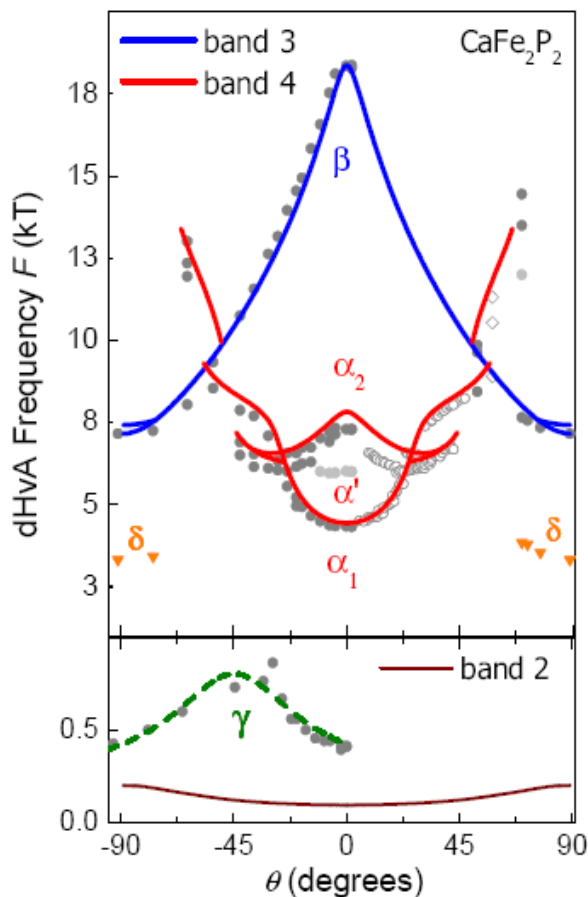
Quantum oscillations in CaFe_2P_2



- torque measurements in 45 T at 0.4 K;
- series of different frequencies corresponding to various extremal areas on the Fermi surface;



Quantum oscillations in CaFe_2P_2



- good agreement between the band structure calculations and experimental data; no band shifts required.
- identical mass enhancement on both electron and hole pockets ~ 1.5 ;
- topological change of the Fermi surface;.

The strength of electronic correlations

SC

LaFePO

BaFe2(As_{1-x}P_x)_2

Mass enhancement: $1 + \lambda$

$m^*/m_b \sim 2$. 2 inner electron pocket
2.54 outer electron pocket

λ

1.2
1.54

~ 2

Non
SC

CaFe2P2

BaFe2P2

$m^*/m_b \sim 1.5$ electron/hole pockets

0.5

$m^*/m_b \sim 1.5$ electron pockets

0.5

$$m^*/m_b = (1 + \lambda_{\text{el-ph}})(1 + \lambda_{\text{el-el}}) \sim 1 + \lambda_{\text{el-ph}} + \lambda_{\text{el-el}}$$

electron-phonon coupling

$\lambda_{\text{el-ph}}^{\text{th}} \sim 0.25$ for Fe-pnictides

electron-electron interactions
(nesting, spin fluctuations)

$\lambda_{\text{el-el}} \sim 0.5 - 1.5$

- Magneto-elastic coupling
- large pnictide polarizability:

Summary

- Fermi surface of 122 compounds extremely sensitive to **structural** effects (c/a ratio –uniaxial pressure ?).
- **For small spacer layer or large *d* orbitals** Fermi surface topology is strongly modified (in particular for the hole bands);
- **Anisotropic scattering:** hole pockets affected much more by impurity scattering as compared to the electron pockets; **orbitals?**
- **Shrinking of the Fermi surface** as compared with the band structure calculations –**electronic correlations**;
- Enhanced effective masses and increased FS nesting in LaFePO and BaFe₂(P_{1-x}As_x) – **strength of electronic correlations**;

